A comparative study of nucleation parameterizations: 2. Three-dimensional model application and evaluation

Yang Zhang,[1] Ping Liu,[1,2] Xiao-Huan Liu,[1,3] Mark Z. Jacobson,[4] Peter H. McMurry,[5] Fangqun Yu,[6] Shaocai Yu,[7] and Kenneth L. Schere[7]

Received 5 March 2010; revised 22 June 2010; accepted 1 July 2010; published 29 October 2010.

[1] Following the examination and evaluation of 12 nucleation parameterizations presented in part 1, 11 of them representing binary, ternary, kinetic, and cluster-activated nucleation theories are evaluated in the U.S. Environmental Protection Agency Community Multiscale Air Quality (CMAQ) modeling system version 4.4. The 12–28 June 1999 Southern Oxidants Study episode is selected as a testbed to evaluate simulated particulate matter (PM) number and size predictions of CMAQ with different nucleation parameterizations. The evaluation shows that simulated domain-wide maximum $PM_{2.5}$ number concentrations with different nucleation parameterizations can vary by 3 orders of magnitude. All parameterizations overpredict (by a factor of 1.4 to 1.7) the total number concentrations of accumulation-mode PM and significantly underpredict (by factors of 1.3 to 65.7) those of Aitken-mode PM, resulting in a net underprediction (by factors of 1.3 to 13.7) of the total number concentrations of $PM_{2.5}$ under a polluted urban environment at a downtown station in Atlanta. The predicted number concentrations for Aitken-mode PM at this site can vary by up to 3 orders of magnitude, and those for accumulation-mode PM can vary by up to a factor of 3.2, with the best predictions by the power law of Sihto et al. (2006) (NMB of −31.7%) and the worst predictions by the ternary nucleation parameterization of Merikanto et al. (2007) (NMB of −93.1%). The ternary nucleation parameterization of Napari et al. (2002) gives relatively good agreement with observations but for a wrong reason. The power law of Kuang et al. (2008) and the binary nucleation parameterization of Harrington and Kreidenweis (1998) give better agreement than the remaining parameterizations. All the parameterizations fail to reproduce the observed temporal variations of PM number, volume, and surface area concentrations. The significant variation in the performance of these parameterizations is caused by their different theoretical bases, formulations, and dependence on temperature, relative humidity, and the ambient levels of H_2SO_4 and NH_3. The controlling processes are different for PM number, mass, and surface areas. At urban/rural locations, some PM processes (e.g., homogeneous nucleation) and/or vertical transport may dominate the production of $PM_{2.5}$ number, and emissions, or PM processes, or vertical transport or their combinations may dominate the production of $PM_{2.5}$ mass and surface area. Dry deposition or some PM processes such as coagulation may dominate $PM_{2.5}$ number loss, and horizontal and vertical transport, and cloud processes (e.g., cloud scavenging and wet deposition) may dominate the loss of $PM_{2.5}$ mass and surface area concentrations. Sensitivity simulations show that the PM number and size distribution predictions are most sensitive to prescribed emission fractions of Aitken and accumulation-mode PM and the assumed initial PM size distribution, in addition to different nucleation parameterizations.

Citation: Zhang, Y., P. Liu, X.-H. Liu, M. Z. Jacobson, P. H. McMurry, F. Yu, S. Yu, and K. L. Schere (2010), A comparative study of nucleation parameterizations: 2. Three-dimensional model application and evaluation, *J. Geophys. Res.*, *115*, D20213, doi:10.1029/2010JD014151.

[1]Department of Marine, Earth, and Atmospheric Sciences, North Carolina State University, Raleigh, North Carolina, USA.
[2]School of Environmental Science and Engineering, Shanghai Jiao Tong University, Shanghai, China.
[3]Environment Research Institute, Shandong University, Jinan, China.
[4]Department of Civil and Environmental Engineering, Stanford University, Stanford, California, USA.
[5]Department of Mechanical Engineering, University of Minnesota-Twin Cities, Minneapolis, Minnesota, USA.
[6]Atmospheric Sciences Research Center, State University of New York at Albany, Albany, New York, USA.
[7]Atmospheric Modeling and Analysis Division, U.S. Environmental Protection Agency, Research Triangle Park, North Carolina, USA.

0148-0227/10/2010JD014151

1. Introduction

[2] Three-dimensional (3-D) modeling of particulate matter (PM) properties (e.g., mass, number, and size distribution) is a formidable task because of the complexity of its physical and chemical processes and the demand for large computational resources. While most 3-D air quality models can reproduce the mass concentrations of PM with an aerodynamic diameter less than or equal to 2.5 μm and 10 μm (i.e., $PM_{2.5}$ and PM_{10}) within ~50% of the measurements, accurately simulating particle number concentrations and size distributions remains challenging [*Zhang et al.*, 2006; *Zhang*, 2008]. Numerous global and regional modeling studies focused on particle mass concentrations. Fewer studies simulated particle number concentrations and size distributions on both global [e.g., *Spracklen et al.*, 2005, 2006, 2007, 2008; *Korhonen et al.*, 2008; *Yu and Luo*, 2009] and regional scales [e.g., *Zhang et al.*, 2006, 2010a; *Elleman and Covert*, 2009a, 2009b]. Most aerosol models perform poorly for the particle number concentrations and size distributions for several reasons. For example, the horizontal grid resolution used in most regional models (≥12 km) is too coarse to reproduce point-wise measurements including particle mass and number concentrations. The number of particle size sections or modes used in most models is often too coarse to resolve the particle number concentrations [e.g., *Zhang et al.*, 2004, 2006] despite exceptions for some models [e.g., *Jacobson*, 1999; *Yu and Luo*, 2009]. Assumptions in model inputs and treatments (e.g., assumed primary emission fractions and associated size distributions) and imperfect model treatments used in some models (e.g., the use of a fixed standard deviation for particle size distribution in simulating particle dynamic processes such as coagulation and condensation) usually lead to errors in simulated particle number concentrations and size distributions [*Zhang et al.*, 1999, 2006, 2010a]. Further, one of the large uncertainties in simulating PM number concentrations and size distributions lies in the model treatment of new particle formation processes due to various homogeneous nucleation mechanisms. Use of different nucleation parameterizations in 3-D models introduces significant uncertainties in the predicted $PM_{2.5}$ number production rates and number concentrations [*Zhang et al.*, 1999, 2009a; *Roth et al.*, 2003; *Zhang and Jacobson*, 2005; *Lucas and Akimoto*, 2006; *Elleman and Covert*, 2009a, 2009b; *Yu et al.*, 2010], which in turn affect visibility, aerosol optical properties, cloud condensation nuclei (CCN), and cloud droplet number concentrations (CDNC) [*Malm*, 1979; *McMurry et al.*, 2005; *Seinfeld and Pandis*, 2006; *Spracklen et al.*, 2008; *Yu and Luo*, 2009; *Pierce and Adams*, 2009; *Kuang et al.*, 2009; *Merikanto et al.*, 2009a; *Zhang et al.*, 2009a].

[3] Particles are simulated in the U.S. Environmental Protection Agency (EPA) Community Multiscale Air Quality (CMAQ) modeling system with three lognormally distributed modes: Aitken, accumulation, and coarse modes (correspond to particles with diameters up to approximately 0.1 μm, between 0.1 and 2.5 μm, and between 2.5 and 10 μm, respectively, for mass distribution) [*Binkowski and Roselle*, 2003; *Byun and Schere*, 2006]. CMAQ simulates major aerosol processes including thermodynamic equilibrium for both inorganic and organic PM, gas-to-particle conversion processes such as binary homogeneous nucleation of sulfuric acid and water vapor, and condensation of gases on pre-existing particles and dissolution of gases into cloud droplets, additional PM growth via coagulation, PM production via aqueous-phase chemistry, aerosol scavenged by cloud droplets, and dry and wet deposition. A number of changes have been made in the aerosol dynamic and thermodynamic treatments in CMAQ in the past few years as newer versions are released for public use. While those changes are targeted primarily at improving predictions of aerosol mass concentrations, the model's capability in simulating number concentration and size distribution remains unchanged due mainly to the use of the same homogeneous nucleation parameterization in version 4.4 and newer (although an improved treatment for PM mass concentrations may also help improve the accuracy of PM size distribution). The binary nucleation parameterization of *Kulmala et al.* [1998] is used as a default module in CMAQ version 4.4 and newer to simulate new particle formation. The parameterization of *Harrington and Kreidenweis* [1998] was used as a default module in the older versions of CMAQ [*Binkowski and Roselle*, 2003]. The parameterization of *Kulmala et al.* [1998] was derived based on the classic binary nucleation theory. It predicts binary nucleation rates up to 2–3 orders of magnitude lower than those predicted by its updated version [i.e., *Vehkamäki et al.*, 2002] due to the fact that its derivation contains mistakes in the kinetic treatment for hydrate formation as pointed out by *Vehkamäki et al.* [2002] and *Noppel et al.* [2002]. *Park et al.* [2006] reported that the CMAQ-predicted $PM_{2.5}$ number concentrations with the parameterization of *Kulmala et al.* [1998] were lower by a factor of 1000 than observations in the southeastern United States. *Elleman and Covert* [2009a] compared the CMAQ-predicted number concentrations for Aitken-mode PM with observations obtained for the Pacific Northwest United States and found that CMAQ with the parameterization of *Kulmala et al.* [1998] underpredicted the PM number concentrations by a factor of 10–100.

[4] Following the examination and evaluation of twelve nucleation parameterizations presented by *Zhang et al.* [2010b], nine nucleation parameterizations have been implemented into CMAQ version 4.4 in this work to future study the sensitivity of simulated particle number concentrations from 3-D CMAQ. These include four binary homogeneous nucleation (BHN) parameterizations (i.e., *Pandis et al.* [1994], *Fitzgerald et al.* [1998], *Vehkamäki et al.* [2002], and *Yu* [2008], referred to as PA94, FI98, VE02, YU08, respectively), three ternary homogeneous nucleation (THN) parameterizations (i.e., *Napari et al.* [2002], *Merikanto et al.* [2007] with corrections by *Merikanto et al.* [2009b], and *Yu* [2006], referred to as NA02, ME07, and YU06, respectively), and two power laws representing empirical kinetic or cluster-activated nucleation (i.e., *Sihto et al.* [2006] and *Kuang et al.* [2008], referred to as SI06 and KU08, respectively). The nine parameterizations are evaluated along with two existing BHN parameterizations in CMAQ (i.e., *Kulmala et al.* [1998] and *Harrington and Kreidenweis* [1998], referred to as KU98 and HK98, respectively) through their applications to the summer 1999 Southern Oxidants Study (SOS99) episode. The parameterization of *Wexler et al.* [1994] is examined by *Zhang et al.* [2010b] (part 1 of this paper) but excluded from the 3-D CMAQ application here, because it exceeds the upper limits of nucleation rates under most atmospheric conditions [*Zhang et al.*, 2010b]. While

KU98 and NA02 are also not recommended for 3-D model applications in the *Zhang et al.* [2010b] paper, their work has been used in several recent 3-D model applications. In particular, NA02 gives a seemingly good agreement [e.g., *Gaydos et al.*, 2005; *Jung et al.*, 2008, 2010; *Elleman and Covert*, 2009b] and may be continuously used in the community. On the other hand, as indicated by *Anttila et al.* [2005] and *Merikanto et al.* [2007], the derivation of this parameterization neglected the ammonium bisulfate formation which governs the ternary nucleation process according to the classical theory and such an omission leads to unrealistically high nucleation rates. NA02 is therefore included in this study to evaluate whether it also gives a good agreement with PM number and size distributions observations in the southeastern United States. If this is true, then these results will help illustrate that the selection of an appropriate nucleation parameterization cannot simply be based on whether it gives a good agreement with observations and that more rigorous investigations and assessments on its fundamental theory and scientific soundness are needed. The predicted particle number concentrations and size distributions with those nucleation parameterizations are analyzed and evaluated against available measurements in Atlanta where the nucleation involving H_2SO_4 was observed [e.g., *McMurry et al.*, 2000]. The controlling atmospheric processes in shaping particle size distributions (e.g., mass, number, and surface area) are studied with a process analysis (PA) tool imbedded in CMAQ and additional sensitivity simulations. While such PA has been conducted in several studies [e.g., *Zhang et al.*, 2005, 2007, 2009b; *Yu et al.*, 2008; *Wang et al.*, 2009; *Liu and Zhang*, 2010; *P. Liu et al.*, 2010; *X.-H. Liu et al.*, 2010a], most focus on the mixing ratios of gases and mass concentrations of PM. To our best knowledge, none of the published PA studies focused on PM number concentrations and surface areas.

2. Model Testbed and Experiment Design

[5] The 3-D modeling domain covers the contiguous United States and a small portion of southern Canada and northern Mexico, with a horizontal resolution of 32 km. The vertical resolution is 21 layers from the surface to ~160 mbar. The simulation period is 12–28 June 1999. The meteorological fields were generated by the U.S. EPA Atmospheric Modeling and Analysis Division using the Pennsylvania State University (PSU)/National Center for Atmospheric Research (NCAR) Mesoscale Modeling System Generation 5 Version 3.4 (MM5) with four-dimensional data assimilation (FDDA). The EPA's National Emissions Inventories (NEI) 99 version 3 is used to generate a gridded emission inventory for all gas and primary PM species for the contiguous United States using the Sparse Matrix Operator Kernel Emissions system (SMOKE1.4). The initial conditions (ICONs) and boundary conditions (BCONs) are set to be those of clear tropospheric air conditions as described by *Yu et al.* [2004]. A spin-up period of two days (12–13 June) is used to minimize the influence of ICONs. All simulations use the Statewide Air Pollution Research Center Mechanism (SAPRC99) [*Carter*, 2000] and the AERO3 aerosol module. The meteorological and chemical predictions from the baseline simulation with KU98 were evaluated using available surface, aircraft, and satellite data by *Liu and Zhang* [2010]. Both MM5 and CMAQ perform reasonably well for major meteorological variables (i.e., temperature, relative humidity, wind direction, planetary boundary layer height, and precipitation), surface concentrations of chemical species (i.e., O_3, $PM_{2.5}$, sulfate, and ammonium), and vertical profiles of temperature and sulfur dioxide, although small to moderate biases are found for most variables evaluated. This paper focuses on the analysis and evaluation of the simulation results for PM number, volume, surface areas from the CMAQ simulations with the 11 nucleation parameterizations and 5 additional sensitivity simulations for a 15 day period of 14–28 June 1999.

[6] Only a small fraction of nucleated particles (i.e., <~1.5 nm) will survive the competition between the rates of growth and removal processes and grow to the CCN size (~100 nm). The growth mechanisms of nucleated particles to the minimal detectable particle size (~2–4 nm) and to the CCN size remain unknown and may involve many processes such as condensation of nucleating vapor, activation of soluble vapor, heterogeneous nucleation, charged-enhanced condensation, coagulation, multiphase chemical reactions [*Kulmala et al.*, 2004a], and many species such as H_2SO_4, H_2O, NH_3, aromatic acids, and aminium salt [*Eisele and McMurry*, 1997; *Kulmala et al.*, 2000; *Zhang et al.*, 2004; *Smith et al.*, 2008, 2010]. The growth rate of the nucleated particles to particles at 2–4 nm is estimated to be about 2 nm h^{-1} [*Eisele and McMurry*, 1997], and that of the particles at 2–4 nm to the CCN size is about 1–22 nm h^{-1} [*Kulmala et al.*, 2004b; *Kuang et al.*, 2009]. Such a growth needs to be taken into account when the nucleation parameterizations are used to predict new particle formation rates and their growth into the CCN size in 3-D models. In addition to the uncertainties in the nucleation parameterizations used and aerosol thermodynamic and dynamic processes treated, an additional uncertainty in simulating particle number concentrations lies in whether and how the model treats the growth of particles at different stages before they grow to the simulated smallest size range (i.e., Aitken mode for CMAQ, which is typically considered to contain particles with diameters of 10–100 nm). Recent progress has been made to simulate such a growth using either an empirical growth rate based on measurements [e.g., *Kerminen and Kulmala*, 2002]; or a particle growth module/parameterization [e.g., *Pierce and Adams*, 2007; *Elleman and Covert*, 2009b; *Kuang et al.*, 2009], or explicitly simulating the microphysics of particles from 1 nm to >10 μm using a 3-D chemical transport model with a size-resolved aerosol microphysical module [e.g., *Spracklen et al.*, 2008; *Yu and Luo*, 2009]. CMAQ, however, does not simulate the loss of nucleated particles by collision and the subsequent growth of "survived" particles from 1 nm to Aitken mode, which will introduce inaccuracies and/or uncertainties in the simulated new particle formation rate and the number concentrations and size distribution of $PM_{2.5}$. By assuming a minimal detectable particle diameter of 2 nm, the new particle formation rates calculated by a nucleation parameterization in CMAQ actually represent their upper limits, because the true new particle formation rates should be always smaller than the nucleation rates. As shown by *Zhang et al.* [2010b], the nucleation rates calculated by some parameterizations may exceed an upper limit prediction of collision-controlled nucleation in terms of dimer production

rate and formation rate of particles with 2 nm diameter [*McMurry*, 1980, 1983]. If the mass production rate calculated from the number production rate in CMAQ exceeds the H_2SO_4 vapor production rate, it is then capped by the H_2SO_4 vapor production rate and the number production rate is reset to that based on the H_2SO_4 vapor production rate, assuming that the particles are 2 nm in diameter. This cap is equivalent to the maximum new particle formation rate, Max J, for particles with 2 nm diameter (i.e., J_{2nm}) defined by *Zhang et al.* [2010b]. The production rate of the newly formed particles at 2 nm is then used to solve the rate of change in the number concentrations of Aitken mode following the approach of *Binkowski and Roselle* [2003]. The new particle number and mass concentrations in Aitken mode calculated using this method represent an upper limit estimation because CMAQ neglects the loss of some particles as they grow from 2 nm to 10–100 nm.

[7] Two sets of model experiments are conducted. The first set consists of a baseline simulation with the default nucleation parameterization of *Kulmala et al.* [1998] and 10 alternative parameterizations (i.e., *Harrington and Kreidenweis* [1998], *Vehkamäki et al.* [2002], *Pandis et al.* [1994], *Fitzgerald et al.* [1998], *Yu* [2008], *Napari et al.* [2002], *Merikanto et al.* [2007] with corrections by *Merikanto et al.* [2009b], *Yu* [2006], *Sihto et al.* [2006], and *Kuang et al.* [2008]). The objectives of this set of experiments are to assess the uncertainties with nucleation parameterizations and their relative accuracies in terms of reproducing particle number and size distributions under an urban environment and to make recommendations regarding the appropriateness of their applications under polluted environments. The particle number concentrations and size distributions predicted with different nucleation parameterizations are compared with available observations in the southeastern United States. Several special field studies were carried out in Atlanta, Georgia, to study atmospheric particle formation, evolution, and health effects. These include the Aerosol Research Inhalation Epidemiological Study (ARIES) [*Van Loy et al.*, 2000; *Woo et al.*, 2001] during 1998–2000 and the Aerosol Nucleation and Real Time Characterization Experiment (ANARChE) study of nucleation in August 2002 [*McMurry et al.*, 2005]. These measurements were carried out at the Jefferson Street (JST) site, located about 4 km northwest of downtown Atlanta [*Woo*, 2003]. Size distributions in the 3 nm to 2 μm range were measured and subsequently segregated into three size ranges (i.e., geometric mean diameter < 10 nm, 10–100 nm, and 0.1–2 μm). High concentrations (up to 2.7×10^5 number cm^{-3}) of freshly nucleated 3–10 nm particles have been frequently observed in summer in Atlanta, Georgia [*McMurry et al.*, 2000; *Woo et al.*, 2001]. The enhancement of ultrafine particle concentrations often occurred near noontime and was associated with high solar radiation. It was suggested that these nanoparticles were formed through a photochemically driven collision-controlled nucleation process involving H_2SO_4 [*McMurry et al.*, 2000]. While the derived nucleation rates based on observed particle size distributions and H_2SO_4 vapor concentrations from ANARChE are used in the Part I paper to evaluate simulated nucleation rates from various parameterizations without considering other atmospheric processes, the observed number, surface, and volume concentrations of PM with diameter less than 2 μm (PM_2) from ARIES during the period of 14–28 June 1999 at JST, Atlanta, Georgia, are used to evaluate CMAQ predictions in this paper (note that no derived nucleation rates are available from the ARIES particle size observations). The comparison is conducted between simulated Aitken-mode PM without cutoff in size and observed $PM_{0.1}$ with an upper cutoff diameter of 0.1 μm, between simulated accumulation-mode PM without cutoff in size and observed $PM_{0.1-2}$ with a diameter range of 0.1–2 μm, and between a number of size-resolved bins in the diameter size range with lower and upper cutoff geometric mean diameters of 0.00306 μm and 2 μm, respectively for simulated and observed PM_2,. The first two comparisons represent an approximation because the tails of the lognormal size distributions for Aitken- and accumulation-mode PM extend beyond the cutoff diameters bounded for observed $PM_{0.1}$ and $PM_{0.1-2}$, whereas the last comparison provides the most rigorous size-resolved evaluation.

[8] The second set consists of a simulation with process analysis and five simulations to study the sensitivity of model PM number predictions to several model parameters or processes of interest. The objectives of this set of experiments are to identify the most important processes in controlling particle properties and to estimate uncertainties associated with assumed model parameters/processes that will affect PM number and size predictions for potential model improvements. Important atmospheric processes in determining particle mass, number, and surface area are first identified with the Integrated Process Rate (IPR) of the PA tool for locations representative of remote, rural, and urban conditions. Sensitivity simulations are then conducted to further investigate the model treatments for several atmospheric processes such as emissions and dry deposition and related parameters such as initial PM size distribution, the fractions of Aitken mode PM in total PM emissions, and dry deposition velocity.

3. Comparisons of Model Predictions With Various Nucleation Parameterizations

3.1. Spatial Distribution of Predicted PM Number, Volume, and Surface Area

[9] Figure 1 shows 15 day mean spatial distributions of hourly $PM_{2.5}$ number concentrations from the simulations with the 11 nucleation parameterizations and maximum nucleation rate. The simulation with J_{2nm} gives $PM_{2.5}$ number concentrations of $10^4 - 2.7 \times 10^6$ cm^{-3} over land and 10^3–10^4 cm^{-3} over oceanic areas. Those over land are $10^2$7.5 $\times 10^4$ cm^{-3} for PA94, $10^2 - 2 \times 10^4$ cm^{-3} for FI98, $10^3 - 1.4 \times 10^5$ cm^{-3} for HK98, $10^2 - 4.9 \times 10^3$ cm^{-3} for KU98, $10^2 - 5.2 \times 10^3$ cm^{-3} for VE02, $10^2 - 4.8 \times 10^3$ cm^{-3} for YU08, $10^4 - 1.4 \times 10^6$ cm^{-3} for NA02, $10^2 - 4.8 \times 10^3$ cm^{-3} for ME07, $10^2 - 5.0 \times 10^3$ cm^{-3} for YU06, $10^4 - 1.8 \times 10^5$ cm^{-3} for SI06, and $10^3 - 2.3 \times 10^5$ cm^{-3} for KU08. The large differences among the predicted PM number concentrations are due to differences in theoretical bases, mathematical equations, processes and assumptions considered in various parameterizations to calculate nucleation rates, as described by *Zhang et al.* [2010b]. Those over oceanic areas simulated by various parameterizations are typically in the range of 10^2–10^3 cm^{-3}. According to the magnitude of the predicted PM number concentrations, the 11 parameterizations can be grouped into four distinct subgroups with

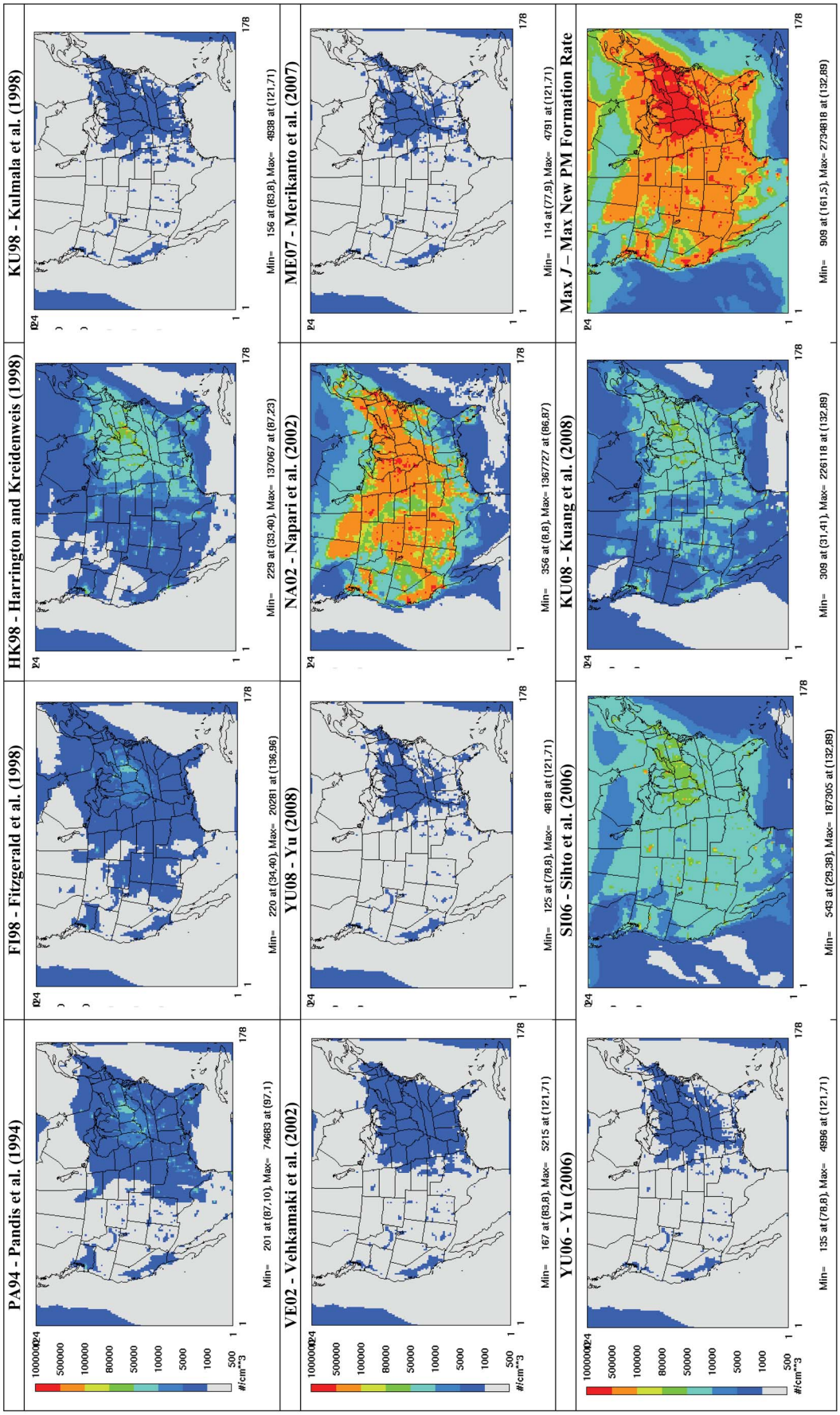

Figure 1. The 15-day average (14–28 June 1999) hourly total number concentrations of $PM_{2.5}$ predicted with the 11 nucleation parameterizations.

values on the order of 10^6 cm^{-3} (i.e., NA02), 10^5 cm^{-3} (i.e., SI06, KU08, and HK98), 10^4 cm^{-3} (i.e., PA94 and FI98), and 10^3 cm^{-3} (i.e., KU98, VE02, YU08, ME07, and YU06) over CONUS. The magnitudes and spatial distributions of volume concentrations simulated by all parameterizations are very similar, ranging from 0.1 to 14.5 μm^3 cm^{-3} (figures not shown). The surface concentrations simulated by all parameterizations have spatial distributions similar to those of number concentrations (figures not shown); and their values are proportional to number concentrations and PM mean diameters, ranging from 3.2 to 379 μm^2 cm^{-3} for NA02, 3.1–350 μm^2 cm^{-3} for SI06, KU08, and HK98, 2.9–327 μm^2 cm^{-3} for PA94 and FI98, and 2.8–290 μm^2 cm^{-3} for KU98, VE02, YU08, ME07, and YU06.

3.2. Temporal Variation of Predicted PM Number, Volume, and Surface Area

[10] Figure 2 shows the predicted number concentrations of Aitken-mode particles at JST, Atlanta, Georgia, and Great Smoky Mountains (GRSM), Tennessee. The number concentrations of observed $PM_{0.1}$ at JST are plotted for an approximate comparison (no observational data are available at GRSM). Note that a logarithmic scale is used to best show the simulated particle number concentrations that vary by several orders of magnitude (10^2 to 10^6 cm^{-3}). Such a log scale somewhat smoothes out the temporal variations of observed particle number concentrations that vary from $>10^2$ to $<10^5$ cm^{-3} throughout the simulation period but only change within 1 order of magnitude during nucleation events (e.g., from 2.5×10^4 to 1.0×10^5 cm^{-3} on 24 June 1999). At JST, the predicted number concentrations for Aitken-mode PM range from 396 to 22661 cm^{-3} by PA94, 432 to 10765 cm^{-3} by FI98, 523 to 243850 cm^{-3} by HK98, 285 to 6010 cm^{-3} by KU98; 297 to 6545 cm^{-3} by VE02, 239 to 2610 cm^{-3} by YU08, 580 to 1674600 cm^{-3} by NA02, 231 to 1169 cm^{-3} by ME07, 269 to 3179 cm^{-3} by YU06, 2284 to 134090 cm^{-3} by SI06, and 656 to 130240 cm^{-3} by KU08. For comparison, the observed number concentrations for Aitken-mode PM at JST range from 2039 to 102309 cm^{-3}. Compared with the observed values, the predicted Aitken-mode PM number concentrations are consistently lower by up to a factor of 96 for PA94, 95 for FI98, 287 for KU98, 276 for VE02, 337 for ME07, 290 for YU06, and 320 for YU08; either higher by up to a factor of 30, 204, 41, and 29 or lower by up to a factor of 81, 97, 25, and 69 for HK98, NA02, SI06, and KU08, respectively. The PM number concentrations from all parameterizations except for NA02 are well below those by the simulation with J_{2nm}, whereas those from NA02 sometime reach or are close to the upper limits. Among all 11 parameterizations tested, the peak number concentrations predicted by the power law of SI06 give the closest agreement to the observed values at JST; the ternary parameterization of NA02, the binary parameterization of HK98, and the power law of KU08 also perform better than other parameterizations in terms of simulated number concentrations. NA02 gives a good agreement in this study and other studies, however, for a wrong reason since it has several fundamental problems/technical flawed treatment as indicated previously and also described in more detail by *Zhang et al.* [2010b], which have been corrected by ME07. The Aitken-mode number concentrations given by ME07 are lower by factors of 1–4246 than those from NA02, which, however, does not reproduce the observed particle number concentrations for the urban environment, due likely to the fact that other nucleation mechanisms may dominate in Atlanta. None of the 11 parameterizations reproduce the temporal variations of the observed $PM_{0.1}$ number concentrations at JST. The simulated PM number concentrations from all parameterizations show a very strong diurnal variation. The peak values occur at noontime when the solar radiation is the strongest and the number concentrations of H_2SO_4 are the maximum, and the values during daytime and nighttime vary by several orders of magnitude. By contrast, the observed values can peak at certain times of a day including both daytime and nighttime (e.g., 1100 LT on 16 and 23 June) and remained high for 2 or more days, the differences between daytime and nighttime values are typically within a factor of 2. The lack of diurnal variations in observed number concentrations indicate that some new particles produced during daytime may remain at night due likely relatively slow removal processes, which are not captured well by CMAQ.

[11] Five parameterizations (i.e., ME07, YU08, YU06, KU98, and VE02) give the lowest number concentrations that differ from the highest number concentrations predicted by SI06 by up to factors of 535 and 496 at GRSM and JST, respectively. The variations in the predicted number concentrations among all parameterizations tested are associated with several factors including the number concentration of H_2SO_4 produced (N_{H2SO4}) via the gas-phase oxidation of SO_2 by OH radicals for all nucleation parameterizations, temperature (T), and relative humidity (RH) for binary and ternary nucleation parameterizations (except for PA94, in which temperature dependence of nucleation rates are not accounted for, and HK98, in which T dependence and RH dependence of nucleation rates are rather weak), and the ambient concentrations of NH_3 (C_{NH3}) for ternary nucleation parameterizations. With a correct kinetic treatment for hydrate formation, VE02 gives nucleation rates slightly higher than those by KU98 (by up to a factor of 2.4 at JST and 2.8 at GRSM) during most time periods. This increase is due mainly to a stronger N_{H2SO4} dependence in work by VE02 [see *Zhang et al.*, 2010b, Figure 1]. In the parameterization of *Vehkamäki et al.* [2002], the nucleation rate is given by an exponential of first- to third-order polynomial of Ln (N_{H2SO4}), whereas that of *Kulmala et al.* [1998] is given by an exponential of first-order polynomial of Ln (N_{H2SO4}). *Yu* [2008] treats the BHN of H_2SO_4 and H_2O as quasi-unary nucleation (QUN) process for H_2SO_4 in equilibrium with H_2O and derive an analytical expression based on a kinetic collision theory to calculate the H_2SO_4–H_2O QUN rate as a function of N_{H2SO4}, T, and RH. *Yu* [2006] calculates the ternary nucleation rates for a system involving H_2SO_4, NH_3, and H_2O using a kinetic THN model with the NH_3 enhancement effect constrained by laboratory experimental results. *Yu* [2008] showed that the QUN rates are lower than those of VE02 that are based on the classical BHN theory; this trend is consistent with the results shown in Figures 1 and 2. *Yu* [2006] reported a negligible contribution of THN rates to new particle formation in the boundary layer, which is also consistent with comparison between observations and simulated values from YU06 in Figure 2. As shown in Figures 1 and 2, NA02 that is based on the classical THN theory gives much higher

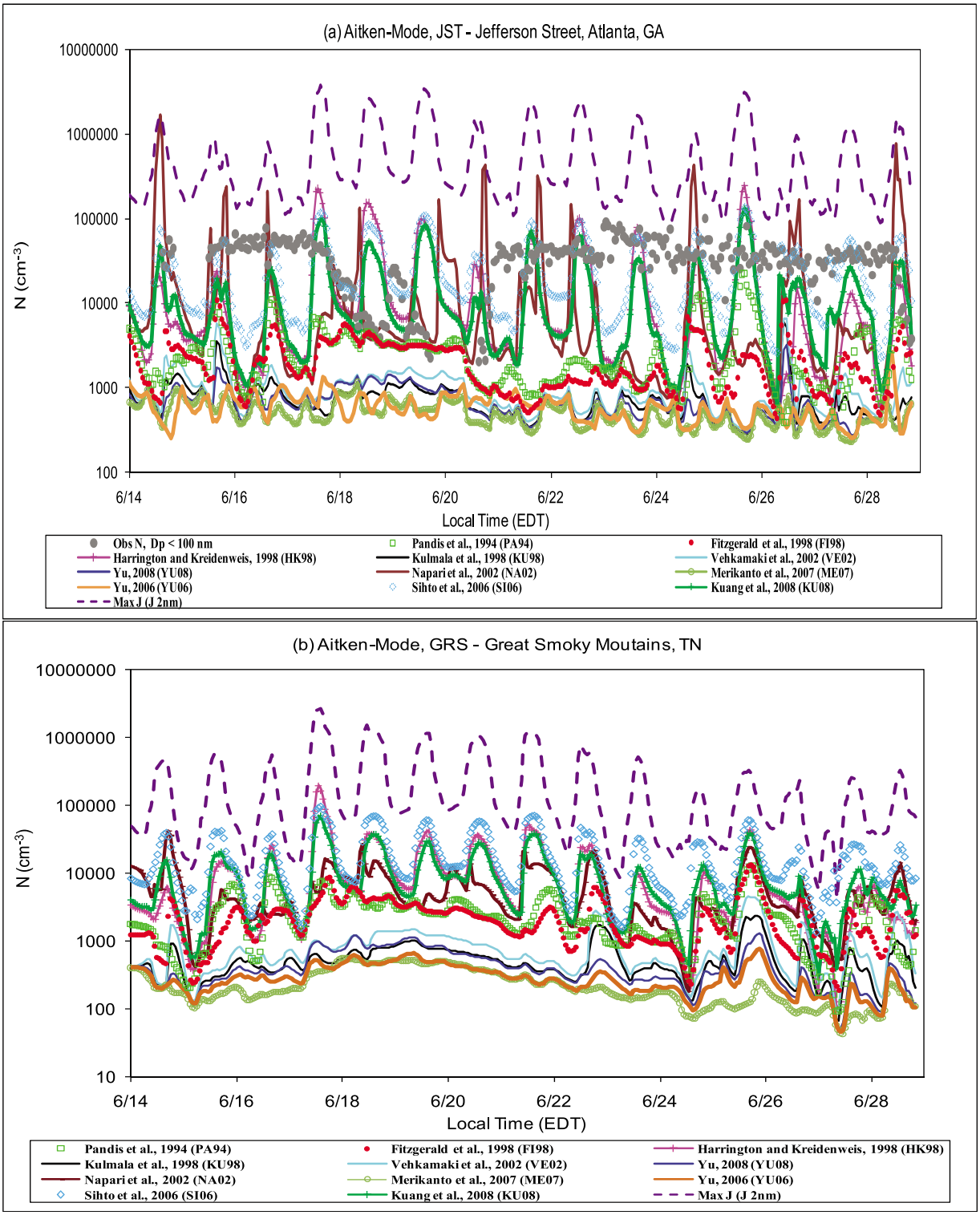

Figure 2. The number concentrations of Aitken-mode particles at (a) JST, Atlanta, Georgia, and (b) the Great Smoky Mountains (GRS), Tennessee, predicted with the 11 nucleation parameterizations. The observational data at JST are obtained for particles with diameter ≤ 100 nm from ARIES. No observational data are available at GRS.

nucleation rates (up to 3 orders of magnitude at JST) than YU06 due to a much higher enhancement in the presence of ppt level of NH_3, whereas the laboratory measurements show only 1 to 2 orders of magnitude enhancement in the presence of several ppt to several ppm level of NH_3 [*Yu*, 2006]. YU06 gives much lower THN rates than NA02 because it uses laboratory data to constrain the rates calculated from the classical THN theory. The predicted N_{H2SO4}

and C_{NH3} are much higher at JST than at GRSM, resulting in much larger amplitudes of the predicted number concentrations among various parameterizations at JST than at GRSM. The PM number concentrations from all parameterizations are well below those by the simulation with J_{2nm} at GRSM. Although no observed PM number concentrations were available for the current model evaluation, some studies have shown that organics may play an important role in the observed nucleation events in the forested region such as GRSM [*Kulmala et al.*, 1998; *Kavouras et al.*, 1998; *O'Halloran et al.*, 2009] due to the availability of high biogenic volatile organic compound (VOC) emissions and resultant concentrations [*Day et al.*, 1997; *Blando et al.*, 1998].

[12] Figure 3 shows the number concentrations of accumulation-mode particles predicted with 11 nucleation parameterizations at JST and GRSM. The number concentrations of observed $PM_{0.1-2}$ at JST are plotted for an approximate comparison. Compared with predicted Aitken-mode PM number, the predicted accumulation-mode PM number concentrations at JST are in much better agreement with the observations despite some overpredictions during most time periods. The predicted number concentrations for accumulation-mode PM range from 269 to 6694 cm^{-3} by PA94, 267 to 6683 cm^{-3} by FI98, 281 to 8665 cm^{-3} by HK98, 266 to 6680 cm^{-3} by KU98, VE02, YU06, YU08, and ME07, 274 to 8013 cm^{-3} by NA02, 271 to 7053 cm^{-3} by SI06, and 269 to 7046 cm^{-3} by KU08. For comparison, the observed number concentrations for accumulation-mode PM at JST range from 254 to 7750 cm^{-3}. Similar to the Aitken-mode predictions, five parameterizations (i.e., KU98, VE02, YU06, YU08, and ME07) give the lowest number concentrations; four parameterizations (i.e., HK98, NA02, SI06, and KU08) give the highest predictions, with a difference by up to factors of 3.2 and 5.4 at GRSM and JST, respectively. The predictions from NA02 sometimes reach or are close to the upper limit of simulated accumulation-mode PM number concentrations using J_{2nm} at both JST and GRSM; the rest of parameterizations are below those limits. The very low number concentrations (<100 cm^{-3}) on 15, 25, and 27 June at GRSM are caused by extremely low H_2SO_4 vapor concentrations during a few midnight to early morning hours (e.g., 0200–0400 LT on 15 June, 0100–0400 LT on 25 June, and 0000–0100 LT on 27 June), mid-afternoon hours (e.g., 1400–1700 LT on 24 June), or morning hours (e.g., 0700–1100 LT on 27 June), as a result of heavy precipitation. Such rain events influence the PM number concentrations simulated by all parameterizations because of their strong dependence on H_2SO_4 vapor concentrations.

[13] Figures 4 and 5 show the observed and predicted volume concentrations and surface area, respectively, for both PM modes at JST. All parameterizations significantly underpredict the volume concentrations for Aitken mode on 14–16 June and 26–28 June but significantly overpredict those on 17–20 June. All parameterizations significantly underpredict the surface areas for Aitken mode during most days except 17–20 June and 25 June. The simulation with J_{2nm} gives much higher surface areas than all nucleation parameterizations for most daytime hours on 17–20, 21–24, and 25 June. During the period of 1300 LT 17 June to 2000 LT 20 June, the predicted H_2SO_4 vapor concentrations are the highest (5.0×10^5 to 2.8×10^8 molecules cm^{-3}, with an average of 7.0×10^7 molecules cm^{-3}), the predicted *RH* values are the lowest (33.2–77.5%, with an average of 54.5%), and the predicted temperatures are in the range of 288–300 K with an average of 294 K. Under these conditions, the new particle formation rates predicted from all parameterizations increase with increasing H_2SO_4 vapor concentrations; increase with increasing *RH* except for NA02; and decrease with increasing *T* (except for PA94, SI06, and KU08, which do not depend on *T*). The H_2SO_4 dependence dominates, resulting in a significant increase of Aitken-mode PM mass concentration, thus high volume concentrations and surface areas of Aitken-mode PM. The overpredictions in the volume concentrations and surface areas of Aitken-mode PM are therefore likely due to the participation of excessive amounts of H_2SO_4 vapor concentrations in nucleation (rather than condensation) during this time period. The volume concentrations and surface areas for accumulation mode are significantly underpredicted on 14–19 June and 21–24 June. An evaluation of predicted 24 h average sulfate concentrations against the observations from SOS99 showed a significant overprediction (by a factor of 2–3) on 19–25 June and a slight underprediction (by 5–7%) on 14–17 June [*Liu and Zhang*, 2010]. The simulated cloud fraction and liquid water content were low during 19–25 June, indicating that the photochemical oxidation of SO_2 rather than aqueous-phase oxidation of SO_2 dominates the formation of H_2SO_4 thus sulfate. The overprediction in sulfate during this time period thus indicates a sufficient amount of H_2SO_4 for nucleation (neither observed temperatures and RHs nor hourly H_2SO_4 or sulfate concentrations are available for model evaluation during this time period). The underpredictions in volume and surface area concentrations for accumulation-mode PM are indeed caused by underpredictions in other PM species such as organic and black carbon [*Liu and Zhang*, 2010]. In addition to uncertainties in predicted meteorology (e.g., higher simulated wind speeds and PBL height than observations as shown by *Liu and Zhang* [2010]), several factors may contribute to such underpredictions. For example, these may include the uncertainties in the emissions of black carbon, primary organic carbon, and precursors of secondary organic aerosols, insufficient condensational growth of PM, uncertainty in the assumed initial size distribution, as well as the use of a 32 km horizontal grid resolution that is too coarse to resolve the local emission strengths and distributions needed to reproduce point-wise observations [*Zhang et al.*, 2006; *Liu and Zhang*, 2010].

[14] For Aitken-mode PM predictions, the simulation with J_{2nm} predicts the highest number concentrations and surface areas but the lowest volume concentrations because it predicts the smallest number and volume mean diameters among all nucleation parameterizations tested. When sufficient H_2SO_4 vapor is available for nucleation (e.g., 17–21 June), ME07 and YU06 give the highest and the second highest number mean diameters, and the highest and the 2nd highest volume mean diameters, resulting in the 5th highest and the 4th highest volume concentrations despite their relative low number concentrations and surface areas. KU98 and VE02 also give high number and volume mean diameters (the 3rd and 4th, respectively, resulting in the 1st and 3rd highest volume concentrations). YU08 gives the second highest volume concentrations. The overpredictions in vol-

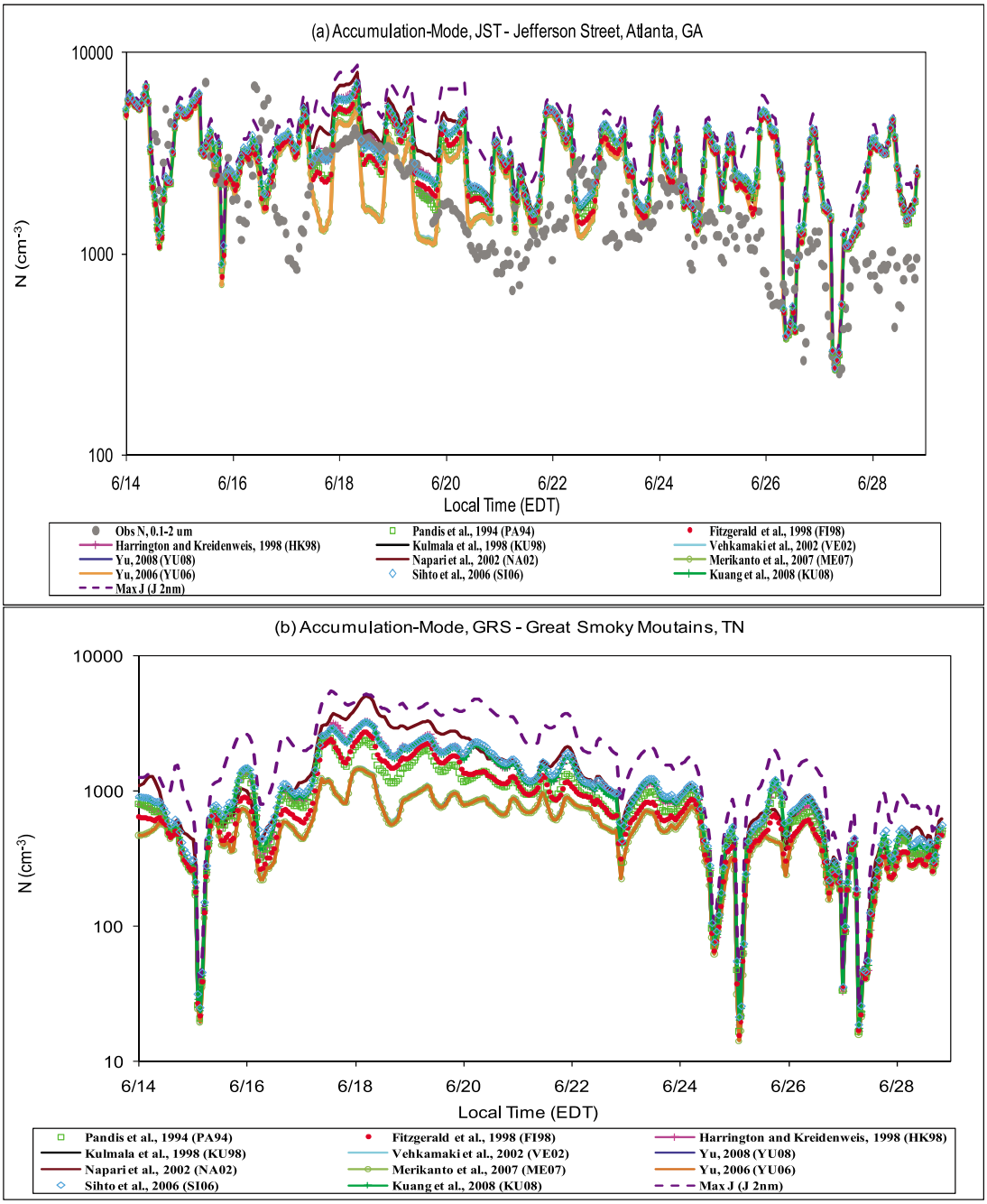

Figure 3. The number concentrations of accumulation-mode particles at (a) JST, Atlanta, Georgia, and (b) the Great Smoky Mountains (GRS), Tennessee, predicted with the 11 nucleation parameterizations. The observational data at JST are obtained for particles with diameter ≤ 100 nm from ARIES. No observational data are available at GRS.

ume concentrations and surface areas by PA94 and FI98 are similar; they are larger than those from HK98, NA02, KU08, and SI06 over most time periods. For accumulation-mode PM, the differences are much smaller in the simulated surface areas and negligible in the simulated volume concentrations predicted by the 11 nucleation parameterizations. None of them reproduce well the temporal variations of volume concentrations and surface areas for both modes during most of time.

3.3. PM Size Distributions

[15] The observed PM_2 number size distributions in Atlanta exhibit three distinct modes, most peaks in the size ranges of 0.00306–0.00406 μm, 0.01863–0.03694 μm, and 0.0499–0.0786 μm (with an exception that the third mode peaks in the range of 0.147–0.242 μm on 18, 20, and 26 June). The observed volume distributions exhibit one to three distinct modes, having one mode on 15, 23, 24, and 27 June, and two modes on 14, 16–22, and 25–27 June and three

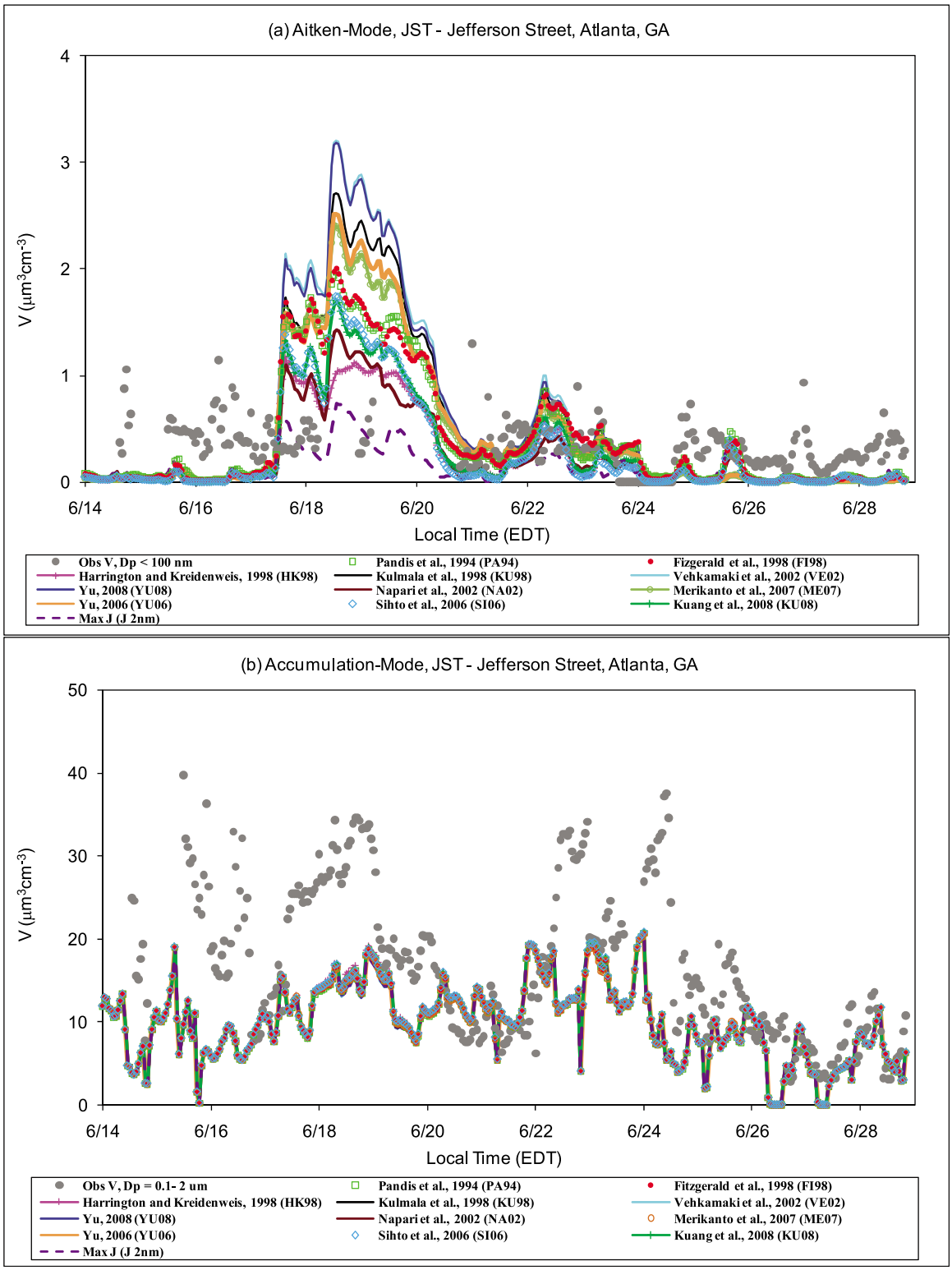

Figure 4. The observed and predicted particle volume concentrations for (a) Aitken mode and (b) accumulation mode at JST, Atlanta, Georgia.

modes on 27 and 28 June. The observed surface area distributions exhibit one to two distinct modes, having one mode on 17–21 and 25 June and two modes on 14–16, 22–24, 26, and 28 June. Figure 6 shows the observed versus predicted 24 h average number, volume, and surface area size distributions on three representative days: 18, 20, and 23 June among the 15 day period. On all three days, KU98, VE02, ME07, YU06, and YU08 reproduce relatively well the number concentrations for the 3rd mode (i.e., the accumulation mode) but significantly underpredict those for the

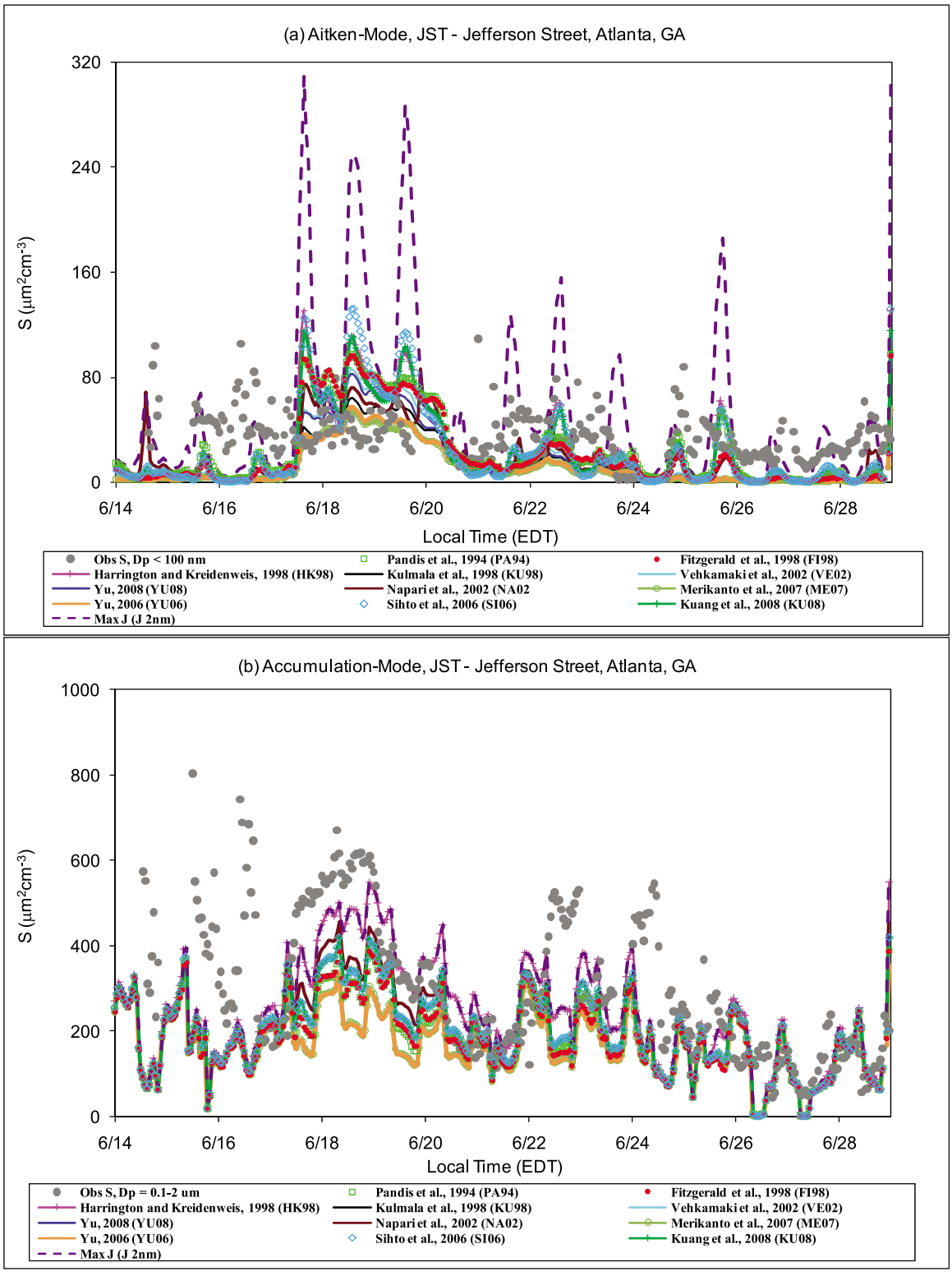

Figure 5. The observed and predicted surface area concentrations for (a) Aitken mode and (b) accumulation mode at JST, Atlanta, Georgia.

1st and 2nd modes (i.e., the nucleation and Aitken modes). PA94 and FI98 also fail to reproduce the 1st mode, but they give slightly better predictions for the 2nd mode than the above five parameterizations. For comparison, HK98, SI06, and KU08 reproduce the number concentrations of the 1st mode to some degrees on all days despite overpredictions (e.g., 18 June) or underpredictions (e.g., 23 June) on some days; they also sometimes underpredict those for the 3rd

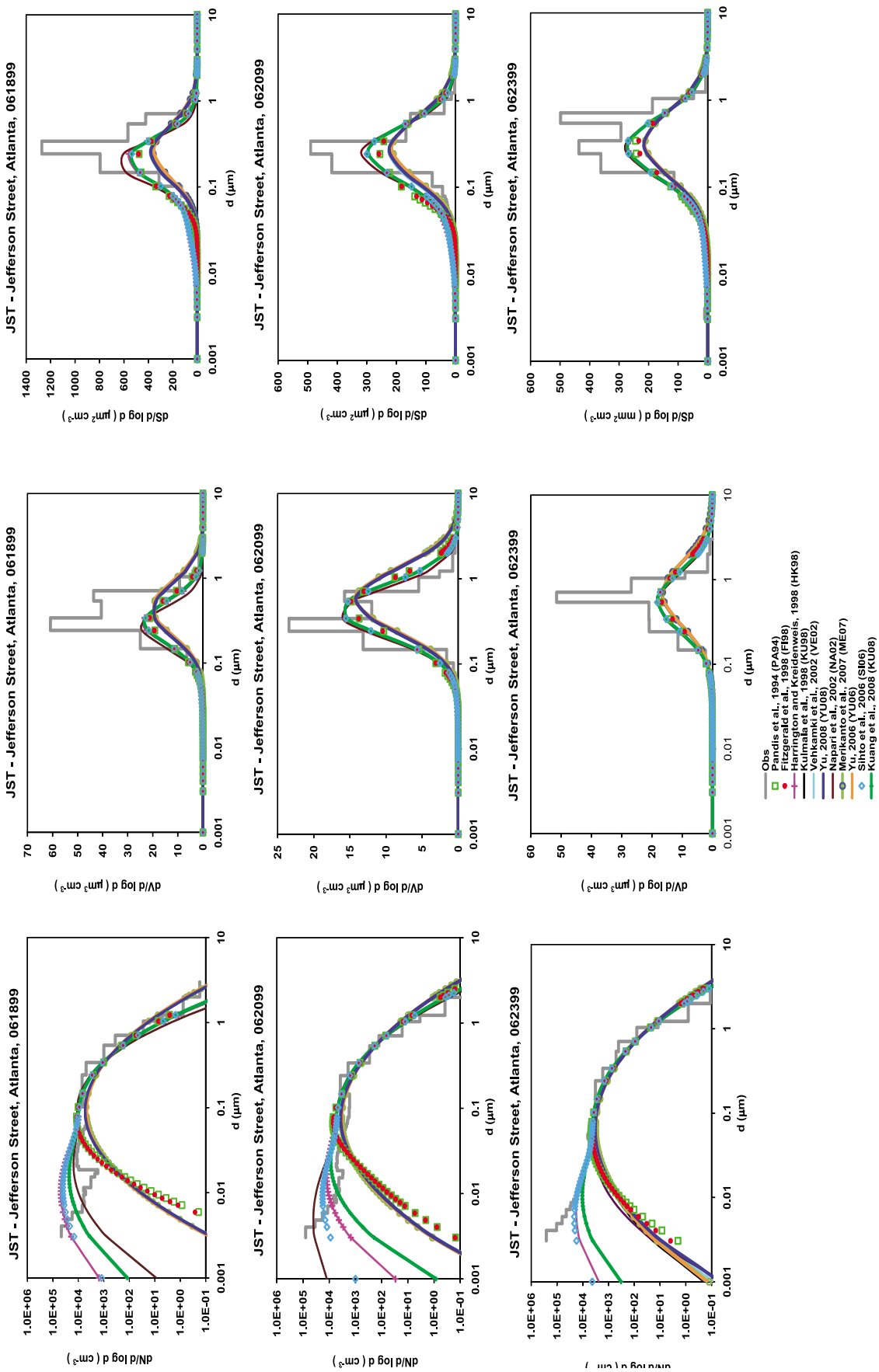

Figure 6. The observed and predicted number, volume, and surface area size distributions at JST, Atlanta, Georgia, on 18, 20, and 23 June 1999.

mode (e.g., on 18 June). NA02 captures well the 2nd mode but also sometimes underpredicts the number concentrations of the 3rd mode (e.g., 18 June); they capture the 1st mode on most days but fail on 17, 23, and 25 June. While all simulations generally reproduce the observed Aitken and accumulation modes whose distributions appear lognormal, the observed size distribution of the nucleation mode is generally poorly characterized because the use of a lognormal distribution in CMAQ cannot well resolve the observed non-lognormal distribution of nanoparticles that are freshly nucleated (typically with a diameter < 5 nm) as reported by *McMurry et al.* [2000] and *McMurry and Woo* [2002]. In addition, the assumption that Aitken-mode particles are produced at the same rate as that of newly formed particles at 2 nm sometimes leads to artificial increases in the number concentrations in the Aitken mode (e.g., 18 and 20 June) and underpredicts those in the nucleation mode (e.g., 18, 20, and 23 June). Considering the loss of nucleated particles by collision and the subsequent growth of "survived" particles from 1 nm to Aitken mode can give more realistic size distributions, as shown by *Elleman and Covert* [2009b]. All parameterizations exhibit a similar underprediction for the volume concentrations and surface areas except on 20–21 and 26–27 June, with the largest mean diameter predicted by ME07 and YU06, and the smallest mean diameter predicted by SI06. These results are quite consistent with the predicted hourly number, volume, and surface areas shown previously.

3.4. Statistical Evaluation

[16] The hourly total number, volume, and surface areas during 14–28 June predicted for $PM_{2.5}$ (i.e., the sum of Aitken and accumulation mode PM) are compared with the observed values for PM_2 using various statistical metrics, as shown in Tables 1a–1c. The simulation with J_{2nm} significantly overpredicts (by a factor of 13.5) the total number concentrations. Seven parameterizations significantly underpredict them (by factors of 14.5, 14.1, 13.7, 13.2, 12.4, 9.2, 7.6, and 1.6 for ME07, YU06, YU08, KU98, VE02, FI98, and PA94, respectively). The remaining four parameterizations also underpredict the total number concentrations but to a much smaller extent (by factors of 2.5, 2.0, 1.6, and 1.5 for KU08, HK98, NA02, and SI06, respectively). While the number concentrations for accumulation-mode PM are overpredicted by factors of 1.4 to 2.2 for all parameterizations, those for Aitken-mode PM are significantly underpredicted by factors of 1.7 to 47 for all parameterizations except for those of NA02 and SI06, resulting in an overall underprediction in the number concentrations of $PM_{2.5}$. The total volume concentrations for $PM_{2.5}$ are underpredicted by factors of ~1.7 by all the parameterizations, largely because the underprediction (by factors of 1.4 to 1.8) in the volume concentrations of accumulation-mode PM overwhelms the overprediction (by factors of 1.2 to 1.6) in the volume concentrations of Aitken-mode PM by all parameterizations except for those of KU08, SI06, NA02, and HK98 (which underpredict the volume concentrations of both Aitken- and accumulation-mode PM by factors of 1.2–1.4 and 1.7–1.8, respectively). The total surface areas are underpredicted by factors of ~1.9 for KU98, VE02, YU08, ME07, YU06, 1.7 for FI98, and PA94, 1.6 for HK98, NA02, KU08, and SI06, and 1.2 for the simulation with J_{2nm}, largely due to the underpredictions in the surface areas of both Aitken- and accumulation-mode PM (by factors of 1.4 to 3.2 and 1.5 to 1.9, respectively) by all nucleation parameterizations. Among the 11 parameterizations, the top four parameterizations having the closest agreement to observations are those of SI06, NA02, HK98, and KU08 for the total number concentrations, and SI06, NA02, KU08, and HK98 for the total surface area concentrations. The performance of all parameterizations in terms of the total volume concentrations is very similar. Overall, SI06 gives the best statistical performance among all parameterizations tested.

[17] A more rigorous evaluation is conducted for the predicted 24 h average number, volume, and surface area size distributions with the 11 nucleation parameterizations by integrating their lognormal size distributions for 39 segregated size sections over the diameter range of 0.001 to 2 μm and then comparing against the ARIES measurements in the diameter range of 0.00306 to 2 μm for PM_2. The upper bound of the observed segregated size sections are 0.00306, 0.00406, 0.0049, 0.00592, 0.00716, 0.00787, 0.00866, 0.00952, 0.01048, 0.01153, 0.01268, 0.01396, 0.01537, 0.01692, 0.01863, 0.02052, 0.02261, 0.02493, 0.02748, 0.03032, 0.03346, 0.03694, 0.04081, 0.0451, 0.0499, 0.056, 0.0609, 0.0663, 0.0722, 0.0786, 0.102, 0.147, 0.242, 0.34, 0.54, 0.71, 1.04, 1.23, and 2.0 μm. Tables 2a–2c show the size-resolved statistics for number, volume, and surface area size distributions over the 15 day period. While the simulation with J_{2nm} overpredicts size-resolved number concentration by a factor of 12.2, other parameterizations underpredict it by factors of 1.3 to 12.4. The size-resolved volume concentrations are underpredicted by factors of 1.8–2.0. The size-resolved surface areas are underpredicted by factors of 2.1 for ME07, KU98, and VE02, 2.0 for YU08 and YU06, 1.8 for FI98 and PA94, 1.6 for HK98, NA02, and SI06, 1.3 for KU08 and the simulation with J_{2nm}. Among the 11 parameterizations, the top four parameterizations having the closest agreement to observations are those of NA02, SI06, HK98, and KU08 for the size-resolved number concentrations, SI06, KU08, HK98, and NA02 (note that YU06 and YU08 also rank the 4th) for the size-resolved volume concentrations, and KU08, SI06, NA02, and HK98 for the size-resolved surface area concentrations. Overall, SI06 gives the best performance for all three size-resolved variables evaluated. These results are quite consistent with the statistics obtained with the total number and surface areas shown in Tables 1a and 1c. The evaluation of size-resolved volume concentrations can discern the performance of various parameterizations better than the evaluation of the total volume concentrations which gives nearly identical performance for all parameterizations.

4. Process and Sensitivity Studies for Controlling Processes

4.1. Process Analysis

[18] Process analysis embedded in CMAQ includes two components: the integrated process rate (IPR) and the integrated reaction rate (IRR). The IPR analysis is conducted to quantify the relative contributions of major atmospheric processes to PM mass, number, and surface areas. Tables 3a–3c summarizes the 15 day average hourly changes in PM

Table 1. Performance Statistics for Hourly $PM_{2.5}$ Number, Volume, and Surface Areas Predicted by CMAQ With Various Nucleation Parameterizations and by Sensitivity Simulations at the Surface Layer During 14–28 June 1999: Number[a]

	PA94	FI98	HK98	KU98	VE02	YU08	NA02	ME07	YU06	SI06	KU08	Initsize	Emisfrac	Emisadj	Lowdepo	Combined	Max *J*
									Number								
MeanObs	43275	43275	43275	43275	43275	43275	43275	43275	43275	43275	43275	43275	43275	43275	43275	43275	43275
MeanMod	5699	4704	21241	3289	3489	3163	26999	2996	3071	29562	17332	38052	51993	28958	29555	43952	584767
Data number	262	262	262	262	262	262	262	262	262	262	262	262	262	262	262	262	262
NMB, %	−86.8	−89.1	−50.9	−92.4	−91.9	−92.9	−37.6	−93.1	−92.7	−31.7	−59.9	−12.1	20.1	−33.1	−30.8	1.6	1251.3
NME, %	86.8	89.1	84.5	92.4	91.9	92.9	110.5	93.1	92.7	63.1	72.9	73.2	51.2	61.7	63.0	60.3	1251.3
NMBF	−6.6	−8.2	−1.0	−12.2	−11.4	−12.7	−0.6	−13.5	−13.1	−0.5	−1.50	−0.1	0.2	−0.5	−0.5	0.02	12.5
NMEF	6.6	8.2	1.7	12.2	11.4	12.7	1.8	13.5	13.1	0.9	1.82	0.8	0.5	0.9	0.9	0.6	12.5
									Volume								
MeanObs	15.93	15.93	15.93	15.93	15.93	15.93	15.93	15.93	15.93	15.93	15.93	15.93	15.93	15.93	15.93	15.93	15.93
MeanMod	9.59	9.58	9.56	9.57	9.57	9.58	9.44	9.58	9.58	9.56	9.57	9.56	9.58	10.39	9.56	10.42	9.50
Data number	244	244	244	244	244	244	244	244	244	244	244	244	244	244	244	244	244
NMB, %	−39.8	−39.9	−40.0	−39.9	−39.9	−39.9	−40.7	−39.9	−39.9	−40.0	−39.9	−40.0	−39.8	−34.8	−40.0	−34.6	−40.4
NME, %	47.0	47.1	47.2	47.1	47.1	47.1	47.7	47.1	47.1	47.2	47.1	47.2	47.1	45.0	47.2	44.9	47.5
NMBF	−0.7	−0.7	−0.7	−0.7	−0.7	−0.7	−0.7	−0.7	−0.7	−0.7	−0.7	−0.7	−0.7	−0.5	−0.7	−0.5	−0.7
NMEF	0.8	0.8	0.8	0.8	0.8	0.8	0.8	0.8	0.8	0.8	0.8	0.8	0.8	0.7	0.8	0.7	0.8
									Surface Area								
MeanObs	309.8	309.8	309.8	309.8	309.8	309.8	309.8	309.8	309.8	309.8	309.8	309.8	309.8	309.8	309.8	309.8	309.8
MeanMod	187.3	180.7	194.5	163.3	165. 8	164.5	195.4	162.1	162.2	196.6	195.0	156.0	220.3	212.3	197.7	188.5	253.7
Data number	244	244	244	244	244	244	244	244	244	244	244	244	244	244	244	244	244
NMB, %	−39.5	−41.7	−37.2	−47.3	−46.5	−47.6	−36.9	−47.7	−46.9	−36.6	−37.1	−48.4	−28.9	−31.5	−36.2	−39.2	−18.1
NME, %	44.6	46.2	42.6	51.1	50.4	51.4	42.8	51.4	50.7	42.3	42.7	49.5	39.1	40.2	42.1	42.8	35.9
NMBF	−0.7	−0.7	−0.6	−0.9	−0.9	−0.9	−0.6	−0.9	−0.9	−0.6	−0.6	−0.9	−0.4	−0.5	−0.6	−0.6	−0.2

[a]PA94, *Pandis et al.* [1994]; FI98, *Fitzgerald et al.* [1998]; HK98, *Harrington and Kreidenweis* [1998]; KU98, *Kulmala et al.* [1998]; VE02, *Vehkamäki et al.* [2002]; YU08, *Yu* [2008]; NA02, *Napari et al.* [2002]; ME07, *Merikanto et al.* [2007]; YU06, *Yu* [2006]; SI06, *Sihto et al.* [2006]; KU08, *Kuang et al.* [2008]. Initsize, Emisfrac, Emisadj, Lowdepo, and Combined denote sensitivity simulations that use work of SI06 but with changes in either model input or process parameters. NMB, NME, NMBF, and NMEF denote normalized mean bias, normalized mean error, normalized mean bias factor, and normalized mean error factor, respectively. An NMBF value of −12.2 means an underprediction by a factor of −13.2 [*Yu et al.*, 2006].

Table 2. Performance Statistics for Size-Resolved Number, Volume, and Surface Area Size Distributions Predicted by CMAQ With Various Nucleation Parameterizations and by Sensitivity Simulations at the Surface Layer During 14–28 June 1999[a]

	PA94	FI98	HK98	KU98	VE02	YU08	NA02	ME07	YU06	SI06	KU08	Init size	Emis frac	Emis adj	Low depo	Combined	Max *J*
									Number								
Mean Obs	1035.7	1035.7	1035.7	1035.7	1035.7	1035.7	1035.7	1035.7	1035.7	1035.7	1035.7	1035.7	1035.7	1035.7	1035.7	1035.7	1035.7
MeanMod	157.4	136.5	599.9	91.1	97.2	86.4	793.5	83.6	83.5	773.2	464.3	959.9	1387.5	766.0	783.9	1155.2	12599.5
Datanumber	585	585	585	585	585	585	585	585	585	585	585	585	585	585	585	585	585
NMB, %	−84.8	−86.8	−42.1	−91.2	−90.6	−91.9	−23.4	−91.9	−91.7	−25.3	−55.2	−7.3	34.0	−26.0	−24.4	11.5	1116.5
NME, %	90.7	91.3	82.1	92.9	92.5	93.0	85.7	93.5	92.8	68.1	78.4	70.2	126.8	69.5	68.2	91.8	1123.1
NMBF	−5.9	−6.6	−0.7	−10.4	−9.7	−11.0	−0.3	−11.4	−11.4	−0.3	−1.2	−0.1	0.3	−0.4	−0.3	0.1	11.2
NMEF	6.0	6.9	1.4	10.6	9.9	11.1	1.1	11.6	11.5	0.9	1.8	0.8	1.3	0.9	0.9	0.9	11.2
									Volume								
	PA94	FI98	HK98	KU98	VE02	YU08	NA02	ME07	YU06	SI06	KU08	Initsize	Emisfrac	Emisadj	Lowdepo	Combined	Max *J*
MeanObs	0.46	0.46	0.46	0.46	0.46	0.46	0.46	0.46	0.46	0.46	0.46	0.46	0.46	0.46	0.46	0.46	0.46
MeanMod	0.24	0.24	0.26	0.24	0.24	0.25	0.25	0.23	0.25	0.256	0.26	0.26	0.26	0.28	0.26	0.28	0.24
Data #	585	585	585	585	585	585	585	585	585	585	585	585	585	585	585	585	585
NMB, %	−47.9	−48.0	−44.8	−49.1	−49.3	−45.8	−45.6	−49.6	−45.7	−44.7	−44.7	−44.4	−44.5	−40.1	−44.7	−39.6	−47.7
NME, %	66.5	67.0	61.7	71.3	69.1	70.0	60.4	72.1	69.0	61.3	61.5	68.0	61.5	59.9	61.0	67.0	57.9
NMBF	−0.9	−0.9	−0.8	−1.0	−1.0	−0.8	−0.8	−1.0	−0.9	−0.8	−0.8	−0.8	−0.8	−0.7	−0.8	−0.7	−0.9
NMEF	1.3	1.3	1.1	1.4	1.4	1.3	1.1	1.4	1.3	1.1	1.1	1.2	1.1	1.0	1.1	1.1	1.1
									Surface Area								
MeanObs	9.06	9.06	9.06	9.06	9.06	9.06	9.06	9.06	9.06	9.06	9.06	9.06	9.06	9.06	9.06	9.06	9.06
MeanMod	5.07	4.95	5.52	4.32	4.40	4.58	5.55	4.29	4.49	5.56	6.92	4.59	6.17	5.98	5.59	5.35	6.96
Data #	585	585	585	585	585	585	585	585	585	585	585	585	585	585	585	585	585
NMB	−44.0	−45.4	−39.1	−52.3	−51	−50.4	−38.8	−52.7	−49.5	−38.6	−23.6	−49.4	−31.8	−34.0	−38.3	−41.0	−23.1
NME	59.1	60.3	54.1	64.9	64	63.2	51.2	65.4	62.1	53.6	66.8	68.1	57.2	52.1	53.0	66.2	59.7
NMBF	−0.8	−0.8	−0.6	−1.1	−1.1	−1.0	−0.6	−1.1	−1.0	−0.6	−0.3	−1.0	−0.8	−0.5	−0.6	−0.7	−0.3
NMEF	1.1	1.1	0.9	1.4	1.3	1.2	0.8	1.4	1.3	0.9	0.9	1.4	0.8	0.8	0.9	1.1	0.8

[a]PA94, *Pandis et al.* [1994]; FI98, *Fitzgerald et al.* [1998]; HK98, *Harrington and Kreidenweis* [1998]; KU98, *Kulmala et al.* [1998]; VE02, *Vehkamäki et al.* [2002]; YU08, *Yu* [2008]; NA02, *Napari et al.* [2002]; ME07, *Merikanto et al.* [2007]; YU06, *Yu* [2006]; SI06, *Sihto et al.* [2006]; KU08, *Kuang et al.* [2008]. Initsize, Emisfrac, Emisadj, Lowdepo, and Combined denote sensitivity simulations that use work of SI06 but with changes in either model input or process parameters. NMB, NME, NMBF, and NMEF denote normalized mean bias, normalized mean error, normalized mean bias factor, and normalized mean error factor, respectively. An NMBF value of −5.9 means an underprediction by a factor of −6.9 [*Yu et al.*, 2006].

Table 3. The 15 Day Average (14–28 June 1999) Changes in PM Number, Mass, and Surface Areas of Aitken- and Accumulation-Mode Particles Due To Seven Major Atmospheric Processes at JST, Atlanta, GA, Los Angeles (LAX), CA, and GRS, TN

	Location	Horizontal Transport	Vertical Transport	Emissions	Dry Deposition	PM Processes	Cloud Processes	Mass Balance Adjustment
				Changes in PM Number Concentrations (cm^{-3} h^{-1})				
Aitken	JST	−2.2E+02	6.1E+01	1.5E+01	−1.4E+03	2.6E+03	−1.1E+03	−1.5E+01
	LAX	−3.9E+04	7.8E+02	1.8E+01	−4.8E+04	8.6E+04	−2.3E+01	−3.2E+02
	GRSM	3.3E+02	6.3E+02	2.9E−01	−9.3E+01	−1.0E+03	1.3E+02	1.0E+01
Accumulation	JST	−6.2E+01	−2.9E+00	1.0E+02	−3.8E+00	−7.0E+00	−3.0E+01	−4.3E−01
	LAX	−1.1E+02	1.4E+01	7.0E+01	−8.0E+00	3.2E+01	−5.3E−01	−1.1E+00
	GRSM	−7.3E+00	2.3E+01	1.5E+00	−2.1E+00	−6.0E+00	−1.2E+01	2.1E+00
				Changes in PM Mass Concentrations (mg m^{-3} h^{-1})				
Aitken	JST	−4.6E−05	−1.1E−05	1.3E−06	−6.4E−06	1.0E−04	−3.9E−05	−2.4E−06
	LAX	−2.4E−05	1.1E−05	1.5E−06	−9.3E−07	1.2E−05	−7.1E−08	−3.6E−07
	GRSM	−1.0E−04	7.8E−05	2.1E−08	−6.6E−06	6.9E−05	−6.2E−05	1.5E−05
Accumulation	JST	−4.5E−03	−4.0E−04	3.5E−03	−8.0E−05	1.9E−03	−3.9E−04	−2.2E−05
	LAX	−3.5E−03	3.8E−04	2.4E−03	−5.9E−05	7.9E−04	4.2E−05	−6.1E−05
	GRSM	−1.1E−03	1.1E−03	5.3E−05	−7.7E−05	5.8E−04	−6.3E−04	1.3E−04
				Changes in PM Surface Areas (mm^2 cm^{-3} h^{-1})				
Aitken	JST	−1.7E−02	−2.5E−02	1.4E−02	−9.9E−02	4.6E−01	−3.5E−01	−4.7E−03
	LAX	−2.1E+00	1.6E−01	1.6E−02	−1.7E+00	3.7E+00	−2.9E−03	−2.1E−02
	GRSM	7.0E−02	2.9E−01	2.7E−04	−7.8E−02	2.9E−02	−3.6E−01	3.4E−02
Accumulation	JST	−3.9E+00	−2.4E−01	4.3E+00	−1.0E−01	1.1E+00	−1.2E+00	−2.8E−02
	LAX	−4.3E+00	4.1E−01	2.9E+00	−1.1E−01	1.0E+00	−6.6E−03	−5.8E−02
	GRSM	−1.0E+00	1.2E+00	6.4E−02	−7.5E−02	3.9E−01	−7.0E−01	1.5E−01

number, mass, and surface areas concentrations of Aitken- and accumulation-mode PM (referred to as PM-AIT and PM-ACC, respectively) in the planetary boundary layer (PBL) (i.e., model layers 1–14, corresponding to 0 to ~2.5 km) due to seven major atmospheric processes at JST, Atlanta, Georgia, Los Angeles (LAX), California, and GRSM, Tennessee. The seven major atmospheric processes include horizontal transport, vertical transport, emissions, dry deposition, PM processes, cloud processes, and mass balance adjustment. PM processes represent the net effect of PM thermodynamics, new particle formation due to homogeneous nucleation, gas-to-particle mass transfer, condensation of H_2SO_4 and organic compounds on preexisting particles, and coagulation in and between Aitken and accumulation modes. Cloud processes represent the net effect of cloud attenuation of photolytic rates, convective and nonconvective mixing and scavenging by clouds, aqueous-phase chemistry, and wet deposition. The mass balance adjustment corrects the species mass inconsistency and imbalance caused by highly parameterized physical and cloud algorithms such as advection scheme.

[19] At JST, the production of PM-AIT number is dominated by PM processes (2.6×10^3 cm^{-3} h^{-1} or by 97.2%), and its loss is dominated by dry deposition (-1.4×10^3 cm^{-3} h^{-1} or −51.6%) and cloud process (-1.1×10^3 cm^{-3} h^{-1} or −39.8%). Although intramode and intermode coagulation plays an important role to its loss, the production of new particles through homogeneous nucleation is greater than this loss, resulting in a net production due to PM processes. The controlling processes for PM-ACC number are quite different, with primary emissions as the only production process (1.0×10^2 cm^{-3} h^{-1} or 100%) and horizontal transport and cloud processes (−62 cm^{-3} h^{-1} or −58.3% and −30 cm^{-3} h^{-1} or −28.3%, respectively) dominating its loss. The contributions of PM processes and dry deposition to its loss are relatively small (−6.6% and −3.4%, respectively). The loss processes such as coagulation within PM-ACC and between PM-AIT and PM-ACC dominate over the gain processes such as the growth of PM-AIT via gas-to-particle conversion and self-coagulation of PM-AIT to form PM-ACC, leading to a small net loss due to PM processes. At LAX, PM processes also dominate the production of PM-AIT number concentrations (8.4×10^4 cm^{-3} h^{-1} or 99.1%), and dry deposition and horizontal transport dominate its loss (-4.8×10^4 cm^{-3} h^{-1} or −54.8% and -3.9×10^4 cm^{-3} h^{-1} or −44.8%, respectively), reflecting the influences of dry weather conditions and sea breezes. For PM-ACC number, emissions, PM processes, and vertical transport contribute to its production at rates of 70, 32, and 14 cm^{-3} h^{-1} (or 60.7%, 27.5%, and 11.8%), respectively, and horizontal transport and dry deposition contribute to its loss at rates of −110 (or −91.8%) and 8 cm^{-3} h^{-1} (or −6.8%), respectively. The dominant processes are quite different at GRSM, a remote mountain site that is affected by long-range transport of air pollutants from upwind urban locations. The production of PM-AIT number is controlled by vertical transport, horizontal transport, and cloud processes with rates of 6.3×10^2, 3.3×10^2, and 1.3×10^2 cm^{-3} h^{-1} (or 57.3%, 30.7%, and 11.7%), respectively. Its loss is controlled by PM processes (-1.0×10^3 cm^{-3} h^{-1} or −91.7%) and dry deposition (−93 cm^{-3} h^{-1} or −8.3%). At this site, coagulation (rather than homogeneous nucleation) dominates because of lack of sources of H_2SO_4 for nucleation, resulting in a net loss due to PM processes. Vertical transport also contributes predominantly (23 cm^{-3} h^{-1} or 86.3%) to the production of PM-ACC number. Processes contributing to its loss include cloud processes (−12 cm^{-3} h^{-1} or −44.5%), horizontal transport (−7.3 cm^{-3} h^{-1} or −26.4%), PM processes (−6.0 cm^{-3} h^{-1} or −21.6%), and dry deposition (−2.1 cm^{-3} h^{-1} or −7.5%).

[20] While PM processes (e.g., homogeneous nucleation) provide a dominant source for PM-AIT mass concentration

at JST (1.0×10^{-4} μg m^{-3} h^{-1} or 98.8%), both PM processes (1.2×10^{-5} μg m^{-3} h^{-1} or 49.4%) and vertical transport (1.1×10^{-5} μg m^{-3} h^{-1} or 44.6%) are important sources of PM-AIT at LAX. While horizontal transport dominates its loss at LAX (-2.4×10^{-5} μg m^{-3} h^{-1} or −94.6%), several processes including horizontal transport, cloud processes, and vertical transport provide important sinks at JST (-4.6×10^{-5}, -3.9×10^{-5}, and -1.1×10^{-5} μg m^{-3} h^{-1} or −44%, −36.7%, and −10.9%, respectively). For PM-ACC mass concentration at urban locations, emissions and PM processes dominate their production at rates of 3.5×10^{-3} and 1.9×10^{-3} μg m^{-3} h^{-1} (or 64.8% and 35.2%) at JST and 2.4×10^{-3} and 7.9×10^{-4} μg m^{-3} h^{-1} (or 66.1% and 22.1%) at LAX, respectively. Horizontal transport dominates its loss (-4.5×10^{-3} μg m^{-3} h^{-1} or −83.6% at JST and -3.5×10^{-3} μg m^{-3} h^{-1} or −94.6% at LAX). Compared with LAX, particles at JST have a larger production rate for mass concentrations but smaller number production rates of PM-AIT and PM-ACC. This indicates that particles at JST are larger in size than those at LAX, which is caused by the abundance of sulfate at JST that exists mostly in PM-ACC (0.1–2.5 μm) at JST and that of EC and OM that exist mostly in submicron size range (<~1 μm) at LAX. Dominant processes for PM-AIT and PM-ACC mass concentrations at GRSM are similar to those for PM-AIT at LAX except for a much higher loss rate due to cloud processes (e.g., -6.2×10^{-5} μg m^{-3} h^{-1} or −36.3% at GRSM versus -7.8×10^{-8} μg m^{-3} h^{-1} or −0.3% at LAX for PM-AIT), due to stronger cloud scavenging at GRSM than at LAX. This leads to a lower percentage contribution of horizontal transport to the total loss rate at GRSM (−59.8%) than at LAX (−94.6%) for PM-AIT. The large differences in controlling processes of PM-ACC mass concentrations at urban and rural locations attest a need to develop region-specific (rather than cross-broad) emission control strategies, with a focus on primary PM emissions from local sources in urban areas and those from upwind sources in rural areas. Controlling the emissions of precursors of secondary PM in both rural and urban areas will also be effective. Reduction in primary PM emissions can lead to reduction in secondary PM through reducing the total surface areas available for the heteorogeneous reactions to produce sulfate and nitrate or the secondary organic matter formation through reducing the mass concentrations of absorbing primary organic matter that affects the gas/particle partitioning of semivolatile organic compounds. Such emission control strategies should also account for the transport of the PM emissions away from the urban regions under prevailing weather conditions.

[21] Dominant processes for the surface area concentration of PM-AIT and PM-ACC are generally similar to those for their number concentrations at JST and LAX. At GRSM, dominant processes for the surface area concentration of PM-AIT are different from those for its number and mass concentrations and those for PM-ACC are different from the dominant processes for its number concentration but similar to those for its mass concentrations. At GRSM, vertical and horizontal transport dominate the production of PM-AIT surface area concentration (2.9×10^{-1} μm^2 cm^{-3} h^{-1} or 68.7% and 7.0×10^{-2} μm^2 cm^{-3} h^{-1} or 16.5%, respectively), and cloud processes and dry deposition dominate their loss with rates of -3.6×10^{-1} and -7.8×10^{-2} μm^2 cm^{-3} h^{-1} (or −82.3% and −17.7%), respectively. Vertical transport and PM processes dominate the production of PM-ACC surface area at rates of 1.2 and 0.39 μm^2 cm^{-3} h^{-1} (or 66.3% and 22%), respectively, and horizontal transport and cloud processes dominate its loss at rates of −1.0 and −0.7 μm^2 cm^{-3} h^{-1} (or −57.1% and −38.8%), respectively, which are similar to the dominant processes for PM-ACC mass concentrations.

[22] Figure 7 shows the 15 day average percentage contributions of each process to number, mass, and surface area of $PM_{2.5}$ (i.e., the sum of PM-AIT and PM-ACC) in the PBL at two urban (JST and LAX), Figure 8 two rural (Yorkville (YRK), Georgia, and Penn State (PSU), Pennsylvania), and two remote locations (GRSM and Olympic National Park (OLY)). At all sites, controlling processes for $PM_{2.5}$ number concentrations are similar to those for PM-AIT, and those for $PM_{2.5}$ mass concentrations are similar to those for PM-ACC (figures not shown), reflecting the dominance of $PM_{2.5}$ number in PM-AIT and $PM_{2.5}$ mass in PM-ACC. Controlling processes for $PM_{2.5}$ surface areas are dominated by those for PM-ACC at JST and LAX because of its dominance in total $PM_{2.5}$ surface areas and by those for both PM-AIT and PM-ACC at GRSM because of their comparable contributions to total $PM_{2.5}$ surface areas. For the production of $PM_{2.5}$ number concentrations, PM processes is the top contributor due to the dominance of homogeneous nucleation over other PM processes (except at GRSM where vertical transport dominates and PM processes play an opposite role (i.e., lead to a net loss); and horizontal transport may be the second most important process at some rural or remote sites (e.g., OLY and GRSM). For the loss of $PM_{2.5}$ number concentrations, dry deposition is the top contributor at all sites except for GRSM where PM processes dominate, and other processes can sometime be the second largest contributors (e.g., cloud processes at JST and YRK). For production of the $PM_{2.5}$ mass concentrations, emissions are the top contributor at urban sites whereas PM processes are the top contributor at rural sites. Other processes such as vertical and horizontal transport may also be important or even dominate at some sites (e.g., at GRSM and OLY). The important processes to the loss of $PM_{2.5}$ mass concentrations include horizontal transport at urban and some rural sites (e.g., at JST, LAX, YRK, and GRSM), and vertical transport at some rural sites (e.g., PSU and OLY). For $PM_{2.5}$ surface area concentrations, important processes include emissions or PM processes for its production at all sites except at GRSM where vertical transport dominates and at OLY where both PM processes and horizontal transport are equally important. Horizontal transport dominates their loss at urban sites and some rural sites (e.g., at JST, LAX, YRK, and GRSM) and vertical transport dominates their loss at some sites (e.g., OLY), and cloud processes are important loss processes at some sites (e.g., GRSM, YRK, and PSU). Compared with urban and upwind locations, processes contributing to $PM_{2.5}$ number, mass, and surface areas are relatively more complicated at rural/remote and/or downwind locations (e.g., GRSM and OLY).

4.2. Sensitivity Simulations

[23] Given current model deficiency in reproducing PM number concentrations and size distributions, the sensitivity study here is focused on several major factors that likely affect PM number concentrations and size distributions. In

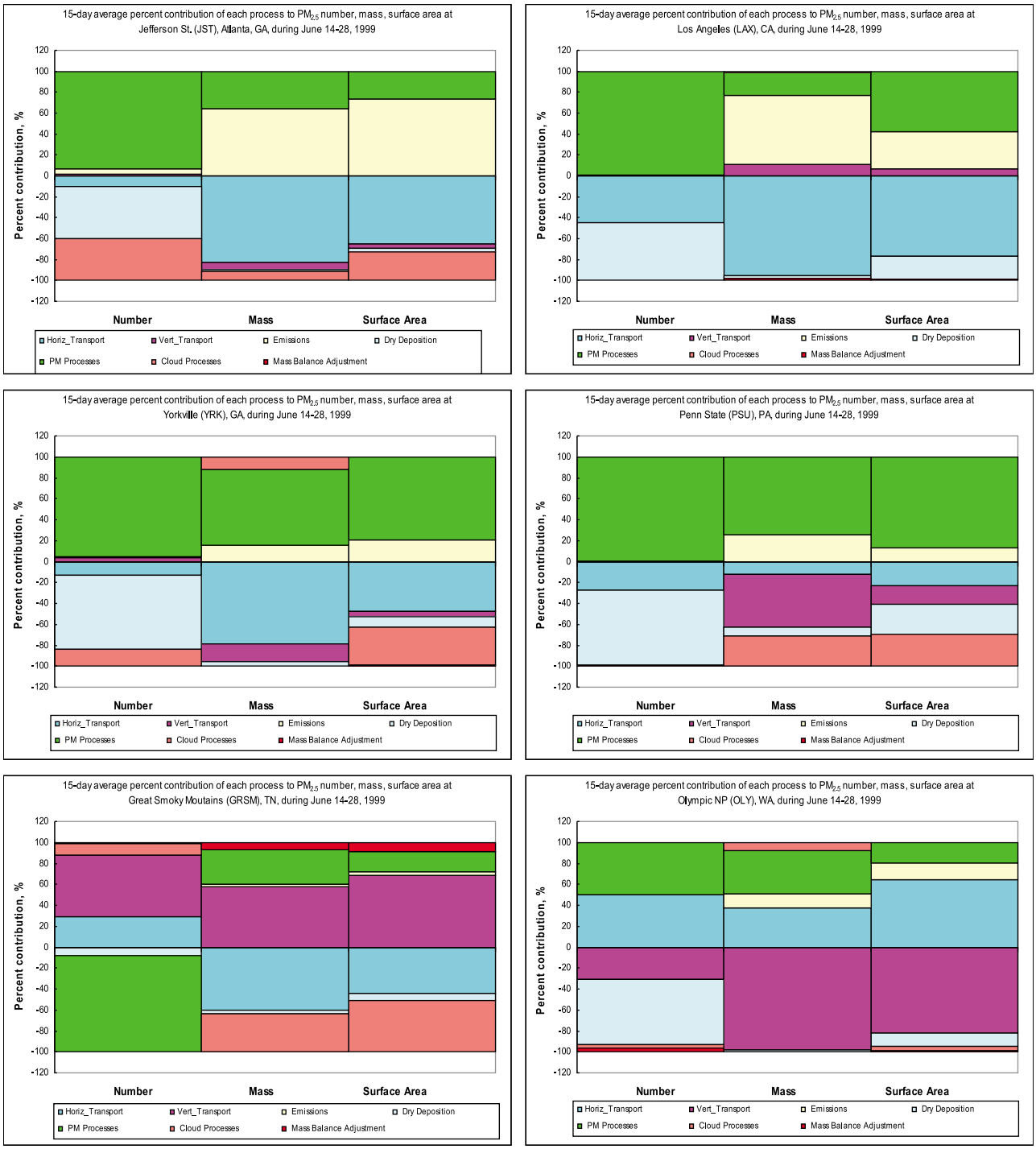

Figure 7. The 15-day average (14–28 June 1999) percentage contributions of each process to number, mass, and surface area of $PM_{2.5}$ (Aitken- and accumulation-mode PM) at two urban sites ((a) JST and (b) LAX), two rural sites ((c) Yorkville (YRK), Georgia, and (d) Penn State (PSU), Pennsylvania), and two remote sites ((e) GRSM and (f) Olympic National Park (OLY)).

addition to homogeneous nucleation, several atmospheric processes such as emission and dry deposition may be important to the predicted PM number concentrations and size distributions, as shown in the above process analysis. Several parameters that may affect PM number emission rates include the assumed initial size distributions for PM emitted, the assumed emission fractions of PM-AIT and PM-ACC in total $PM_{2.5}$ emissions, and the direct emission rates of PM mass. In CMAQ, a constant PM size distribution with d_v of 0.03 μm and σ_g of 1.7 for PM-AIT and d_v of 0.3 μm and σ_g of 2.0 for PM-ACC is assumed based on *Whitby* [1978] to calculate the emission rates for PM number and second moment (i.e., surface area), E_{number} and $E_{surface}$ [*Binkowski and Roselle*, 2003]. The values of d_v and

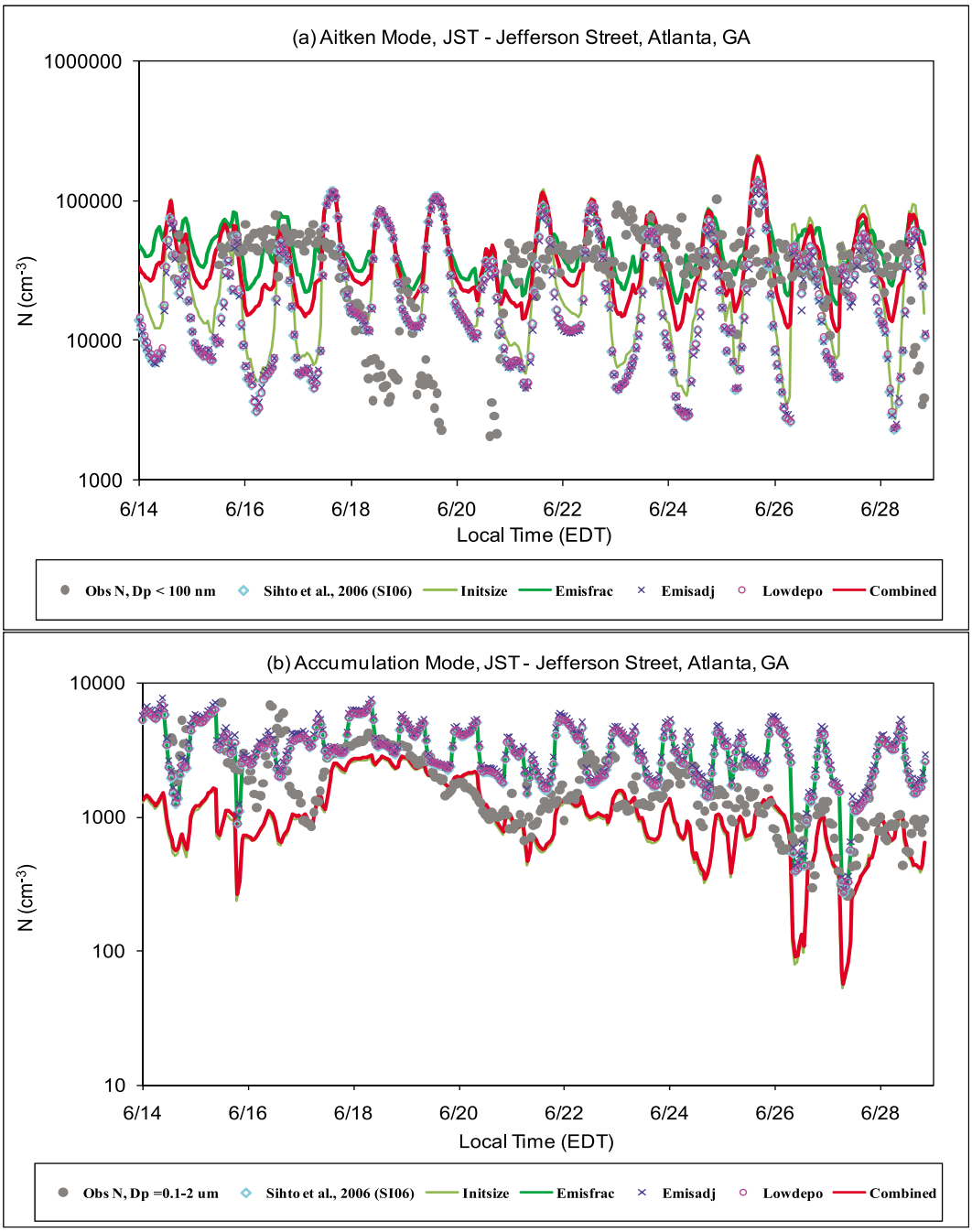

Figure 8. The predicted hourly PM number concentrations for (a) Aitken mode and (b) accumulation mode from the baseline simulation (i.e., SI06) and the five sensitivity simulations (i.e., Initisize, Emisfrac, Emisadj, Lowdepo, and Combined).

σ_g may vary with regions of applications that may have different characteristics of emission and meteorology. In this study, they can be derived from the measured 24 h average PM size distribution by assuming a lognormal distribution which is a plausible assumption for most measurements of Aitken- and accumulation-mode PM size distributions. Based on the ARIES measurements at JST, Atlanta, Georgia, during 12–28 June, the derived values of d_v and σ_g are in the range of 0.0771–0.0925 μm and 2.195–2.6543, respectively, for PM-AIT and 0.285–0.5075 μm and 1.5358–1.7922, respectively, for PM-ACC. The 17 day average values of d_v of 0.0903 μm and σ_g of 2.452 for PM-AIT and d_v of 0.3981 μm and σ_g of 1.6778 for accumulation-mode PM are used in the first sensitivity simulation (referred to as the simulation "Initsize"). Similar sensitivity studies by adjusting the emission size distributions used in CMAQ were conducted by *Park et al.* [2006] and *Elleman and Covert* [2010]. For emission fractions, CMAQ assumes that 99.9% of $PM_{2.5}$ emissions are in PM-ACC for organic and elemental carbon (0.1% in PM-AIT). For other species such as sulfate and other inorganic aerosols, it assumes 100% in PM-ACC [*Binkowski and Roselle*,

2003]. This assumption is based on a field study of on-road emissions of diesel soot conducted by the U.S. EPA (F. S. Binkowski, University of North Carolina at Chapel Hill, personal communication, 2005) and may not be applicable for emissions of all other $PM_{2.5}$ compositions. A sensitivity simulation (referred to as the simulation "Emisfrac") is conducted to investigate this uncertainty. The observed volume concentrations of PM-AIT during ARIES account for 0.5–14.2% of observed total volume concentrations of PM_2. The emission fractions of Aitken- and accumulation-mode PM are therefore assumed to be 10% and 90%, respectively, in this sensitivity simulation. *Liu and Zhang* [2010] evaluated the model performance of CMAQ using observed $PM_{2.5}$ concentrations for the same episode and found that $PM_{2.5}$ concentrations were underpredicted by 10.2–39.0% at various network sites. The concentrations of NO_3^-, BC, and OC were underpredicted by 22.2–77.8%, 34.4–54.9%, and 24.9–58.6%, respectively, and those of SO_4^{2-} were overpredicted by 17.8–20.1%, those of and NH_4^+ were overpredicted by 8.1–24.2% at rural and remote sites but underpredicted by 20.6% at urban and suburban sites over the southeastern United States. By comparing with a more advanced NH_3 inventory, *P. Liu et al.* [2010] reported that the NH_3 emissions based on the NEI v3 used in this study were lower by 25.5% on average domain-wide and an emission adjustment factor of 1.2551 was therefore applied to total NH_3 emission in their sensitivity simulations. Uncertainties also exist in the emissions of primary PM species such as BC and OM [*Zhang et al.*, 2006], which may have contributed to the discrepancies between observed and simulated PM species for this episode. In the 3rd sensitivity simulation, the emissions of primary PM species are therefore adjusted (i.e., increase by 50% for BC and by 40% for OC and NO_3^-, and decrease by −20% for SO_4^{2-}) and the emissions of NH_3 are also increased by 25.51% (referred to as simulation "Emisadj"). In the 4th sensitivity simulation, dry deposition velocities for $PM_{2.5}$ number and surface area are reduced by 20% (referred to as simulation "Lowdepo"). The selection of such a perturbation is based on several considerations. First, no direct measurements of dry deposition velocities for $PM_{2.5}$ number and surface area are available and one must make some assumptions in selecting the value and direction of the perturbation. Second, the dry deposition fluxes of PM number and surface area concentrations are assumed to be controlled by the same processes as PM mass concentrations and the same set of equations is used to calculate dry deposition fluxes of PM mass, number, and surface area concentrations in CMAQ. It is therefore reasonable to assume that the uncertainties in dry depositions of PM number and surface area are the same as or similar to those of PM mass concentrations. Third, *X.-H. Liu et al.* [2010b] and K. Olsen et al. (Fine scale modeling of agricultural air quality over the southeastern united states, Part I. Application and evaluation of two air quality models, manuscript in preparation, 2010) evaluated simulated dry deposition fluxes of several PM species against the calculated values from CASTNET that are based on meteorological measurements and the predictions of the Multilayer Model for a summer episode in the southeastern United States and found that CMAQ underpredicted the dry deposition fluxes of PM species by 80–98%. Fourth, *P. Liu et al.* [2010] conducted sensitivity simulations by changing dry deposition velocity of sulfate by 20% and those of several PM precursors such as SO_2, HNO_3, and NH_3 by 20–50% for the same 12–28 June 1999 SOS episode and found that a perturbation of 20% or larger is needed to predict a sizable change (i.e., > 1–3%) in the simulated PM mass concentrations. Finally, simulated PM number and surface areas from the baseline simulation in this study are underpredicted and using reduced dry deposition velocities may help improve the model predictions. In the 5th sensitivity simulation, all aforementioned changes are combined to estimate the net effects of above changes (referred to as simulation "Combined"). In all five sensitivity simulations, the power law nucleation parameterization of *Sihto et al.* [2006] is used, and the results from those sensitivity simulations are compared with the baseline simulation with the *Sihto et al.* [2006] parameterization (i.e., SI06).

[24] Figures 9, and 10 show the times series plots of the predicted PM number, volume, and surface areas, respectively, for Aitken mode and accumulation mode from the baseline simulation (i.e., SI06) and the five sensitivity simulations. The observations for both modes are also plotted for comparison. Compared with baseline results, adjusting initial size distribution used in calculating PM number and surface area emission rates gives higher number and surface area but lower volume predictions for PM-AIT (the changes are 34.4%, −2.5%, and 5.4%, respectively, on average over hourly predictions on 14–28 June) and slightly higher volume predictions for PM-ACC (by 0.1% on average over hourly predictions on 14–28 June) but lower number and surface area predictions for PM-ACC (by −65.6% and −20.0%, respectively, on average over hourly predictions on 14–28 June). Increasing the emission fraction for PM-AIT from 0.1% to 10% further increases the predicted number, volume, and surface area significantly (by factors of 3.2, 9.9, and 7.9, respectively, on average over hourly predictions on 14–28 June) but has little effect on those for PM-ACC (−2.2%, −1.1%, and −1.1% for predicted number, volume, and surface area, respectively). This indicates that the PM-AIT predictions are sensitive to the changes in both the emission fractions and the initial size distribution used in this study, whereas the PM-ACC number and surface area predictions are more sensitive to the changes in the initial size distribution than those in the emission fractions used, and the PM-ACC volume predictions are relatively insensitive to changes in both parameters. The simulated impact of adjusting initial size distribution of emissions on simulated PM number concentrations is fairly consistent with that reported by *Park et al.* [2006] and *Elleman and Covert* [2010]. Adjusting the emissions of NH_3, BC, and primary OM species decreases PM-AIT number concentrations by −2.7% but increases its volume and surface area concentrations by 4.7% and 3.3%, respectively. It increases PM-ACC number, volume, and surface area concentrations by 8.8%, 8.5%, and 7.9%, respectively. The relatively small net increase in volume concentrations in responses to a moderate-to-large increase in the emissions of NH_3, BC, and primary OM indicates that the PM mass concentrations at JST may be dominated by other primary PM such as other unknown inorganic aerosols and other secondary PM such as secondary organic aerosols and/or uncertainties in meteorological factors (e.g., mixing height and temperature) may be a dominant factor for PM

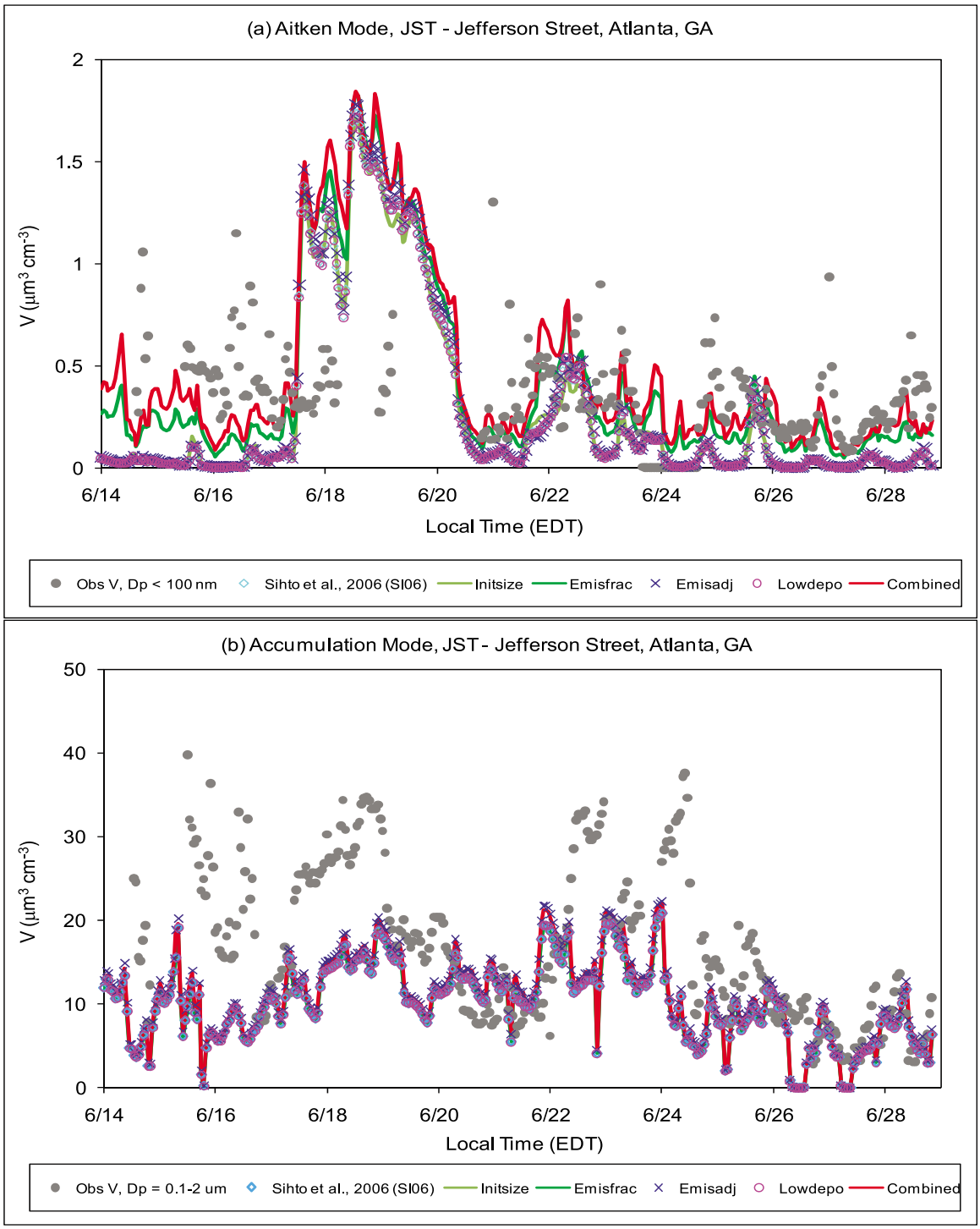

Figure 9. The predicted hourly PM volume concentrations for (a) Aitken mode and (b) accumulation mode from the baseline simulation (i.e., SI06) and the five sensitivity simulations (i.e., Initisize, Emisfrac, Emisadj, Lowdepo, and Combined).

concentrations. Reducing dry deposition velocity by 20% for PM number and surface areas for both modes slightly increases PM-AIT and PM-ACC number concentration (by 1.2% and 0.9%, respectively), PM-ACC volume concentration (0.005%, respectively), and PM-AIT and PM-ACC PM surface area concentration (by 0.5% and 0.6%, respectively), but it slightly decreases the PM-AIT volume concentration (by −0.5%). The simulation that combines all above changes increases the number, volume, and surface area concentrations of PM-AIT by 56.7%, 67.6%, and 88.3%, respectively. It also increases the surface area of PM-ACC by 6.9% but decreases its number and volume concentrations by −63.9% and −15.0%, respectively. Among the five sensitivity simulations, the simulations Initsize and

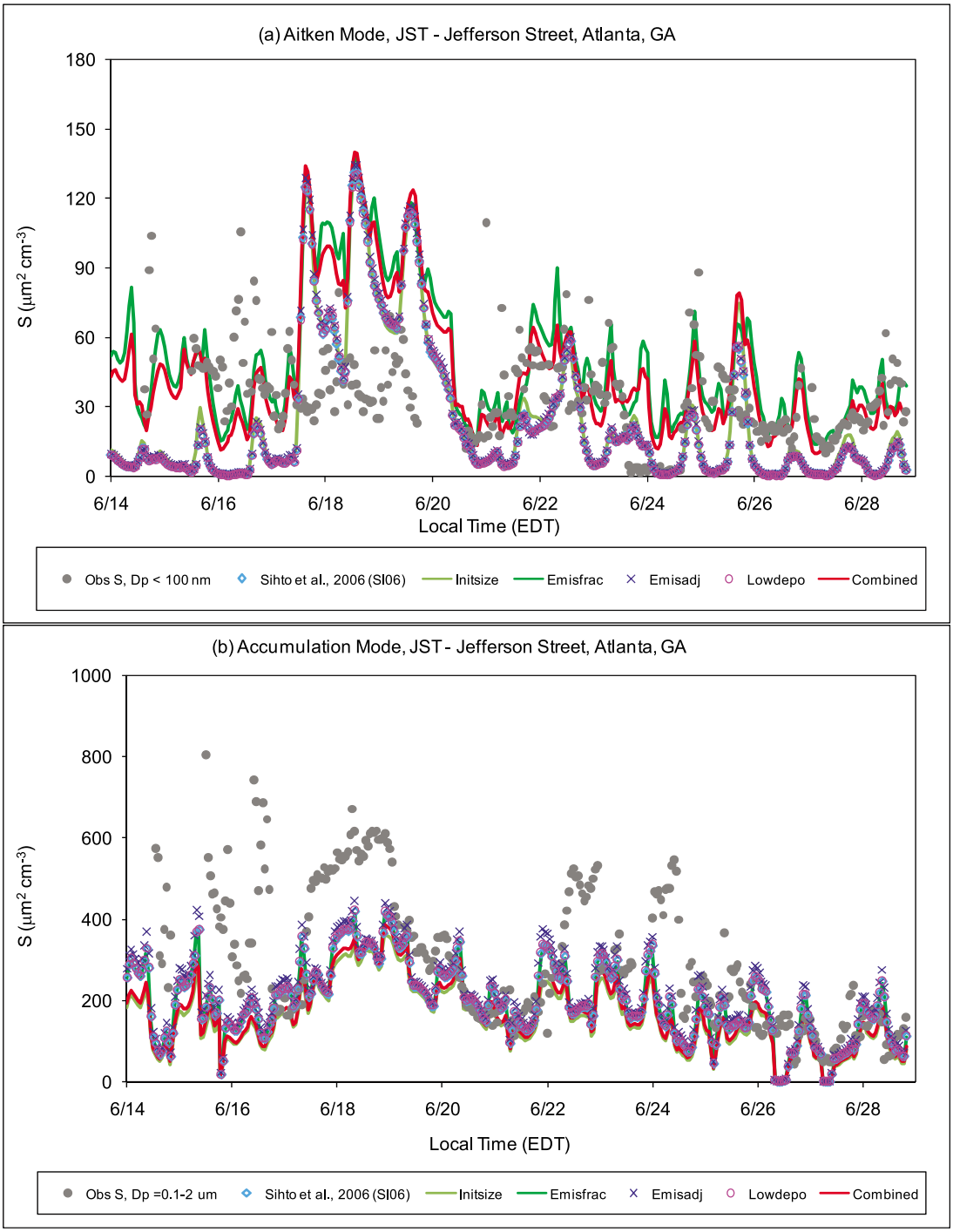

Figure 10. The predicted hourly PM surface concentrations for (a) Aitken mode and (b) accumulation mode from the baseline simulation (i.e., SI06) and the five sensitivity simulations (i.e., Initisize, Emisfrac, Emisadj, Lowdepo, and Combined).

Combined give the closer agreement to the observed temporal variations for number, volume, and surface area predictions for PM-AIT but they both underpredict number and volume concentrations of PM-ACC.

[25] Tables 1a–1c show the statistical measures for predicted total number, volume, and surface area from the five sensitivity simulations. The predicted total $PM_{2.5}$ number concentration changes from ~30000 cm^{-3} for the baseline simulation to ~38000, ~52000, ~29000, ~30000, and ~44000 cm^{-3}, respectively, for simulations Inisize, Emisfrac, Emisadj, Lowdry, and Combined. The increases in Initsize and Emisfrac are compensated by decreases in Emisadj in the simulation Combined, resulting in the closest agreement to the observed number concentration of 43275 cm^{-3} (changing the NMB from −31.7% to 1.6%). Reducing dry deposition velocity by 20% has little effect on

the total PM number predictions. While the changes in the simulations Initsize, Emisfrac, and Lowdepo have little impact on volume concentrations, adjusting emissions in Emisadj and Combined slightly improves them, changing the NMB value from −40% to −35%. The changes in initial size distributions in Initsize and Combined decrease total surface areas (changing NMBs from −36.6% to −48.4% and −39.2%, respectively), and the changes in the simulations Emisfrac and Emisadj increase them (change NMBs from −36.6% to −28.9% and −31.5%, respectively). Tables 2a–2c show statistical measures for size-resolved number predictions from the five sensitivity simulations. Both simulations Initsize and Combined improve the size-resolved number predictions over segregated size sections, changing NMBs from −25.3% to ⁻7.3% and 11.5%, respectively. The simulation Emisfrac increases the NMB from −25.3% to 34%. The changes in simulations Lowdepo and Emisadj have little effects on the size-resolved number predictions.

5. Conclusions

[26] A total of 11 nucleation parameterizations are evaluated in 3-D CMAQ using available measurements from ARIES to assess their appropriateness in reproducing number concentrations and size distributions of $PM_{2.5}$ and the associated uncertainties. Among all parameterizations tested, *Napari et al.* [2002] give the highest number concentrations (by up to the order of 10^6 cm^{-3}), *Sihto et al.* [2006], *Harrington and Kreidenweis* [1998], and *Kuang et al.* [2008] also give high number concentrations (by up to the order of 10^5 cm^{-3}), *Pandis et al.* [1994] and *Fitzgerald et al.* [1998] give moderate number concentrations (by up to the order of 10^4 cm^{-3}), and *Merikanto et al.* [2007], *Yu* [2006, 2008], *Kulmala et al.* [1998], and *Vehkamäki et al.* [2002] predict the lowest number concentrations (by up to the order of 10^3 cm^{-3}). The predicted number concentrations for Aitken-mode PM at JST, Atlanta can vary by up to 3 orders of magnitude, and those for accumulation-mode PM can vary by up to a factor of 3.2. Such a large variation is caused by differences in their theoretical bases, mathematical formulations, different dependence of T, RH, and the ambient levels of H_2SO_4 and NH_3, as well as other processes considered. Compared with the observed values, the total PM number concentrations are significantly underpredicted by all parameterizations, with the best predictions by *Sihto et al.* [2006] (NMB of −31.7%) and the worst predictions by *Merikanto et al.* [2007] (NMB of −93.1%). SI06 also gives the closest agreement to the observed hourly PM number, volume, surface area, and their size distributions at JST among all parameterizations tested, although all the parameterizations fail to reproduce the observed temporal variations of PM number, volume, surface area at JST, Atlanta, Georgia. NA02 gives a good agreement with observed number concentrations but such a good agreement is questionable and warrants further investigations. KU08 and HK98 give better performance than the rest of parameterizations. These results obtained under an urban polluted condition are fairly consistent with the evaluation results under conditions from very clean to highly polluted environments from *Zhang et al.* [2010b]. The simulations with different nucleation parameterizations show large uncertainties in the predicted PM number concentrations and size distributions that will affect model predictions of visibility, aerosol optical properties such as aerosol optical depth (AOD), CCN, and CNDC, demonstrating a need to improve the model's capability in reproducing the PM concentrations and size distributions. Although the current version of CMAQ does not simulate AOD, CCN, and CNDC online, a version of it that is being coupled with the Weather Research and Forecasting model as an online modeling system [*Pleim et al.*, 2008], however, will simulate those parameters that are very important to the accurate predictions of aerosol direct and indirect effects on climate change through modifying atmospheric radiation budgets.

[27] Process analysis shows that controlling processes are different for Aitken mode versus accumulation mode, number versus mass (or volume) versus surface areas, and urban/upwind locations versus rural/remote/downwind locations. At all sites, controlling processes for $PM_{2.5}$ number concentrations are similar to those for Aitken-mode PM, and those for $PM_{2.5}$ mass concentrations are similar to those for accumulation-mode PM. At urban/upwind locations, the production of Aitken-mode number is dominated by PM processes (e.g., homogeneous nucleation) and vertical transport, and its loss is dominated by dry deposition. Horizontal transport and/or cloud processes may play an important role, depending on the meteorological characteristics of the sites. Emission dominates the production of accumulation-mode PM number and the major loss processes may include horizontal transport and cloud processes. Emission dominates the production of accumulation-mode mass concentrations; horizontal transport dominates their losses. Dominant processes for surface areas are generally similar to those for $PM_{2.5}$ number concentrations. At rural/remote and/or downwind locations, vertical and horizontal transport are major production processes for Aitken-mode PM number; and its loss is controlled primarily by PM processes such as coagulation. For accumulation-mode PM number, major production processes may include vertical transport and major loss processes may include cloud processes, horizontal transport, and PM processes. For Aitken- and accumulation-mode mass concentrations, vertical transport and PM processes dominate their production and horizontal transport and cloud processes may dominate their loss. For PM surface areas, vertical and horizontal transport dominate production of Aitken-mode surface areas, and cloud processes and dry deposition may dominate their loss. Vertical transport and PM processes dominate the production of accumulation-mode surface areas and horizontal transport and cloud processes dominate their loss.

[28] Sensitivity simulations provide the relative importance of the assumed initial PM size distribution and several atmospheric processes such as emissions and dry deposition in simulating PM number concentrations and size distributions, in addition to that of the homogeneous nucleation parameterization. Among these processes and parameters, the PM number and size distribution predictions are most sensitive to prescribed emission fractions of Aitken and accumulation-mode PM and the assumed initial PM size distribution, and relatively insensitive to dry deposition and adjustments in emissions of NH_3 and PM species in this study. A simulation that combines all changes increases the predicted total $PM_{2.5}$ number concentration from ~30000 cm^{-3}

for the baseline simulation to ~44000 cm^{-3}, changing the NMB value from −31.7% to 1.6%.

[29] Accurately simulating PM number concentrations and size distributions remain a major challenge because of inaccuracies in primary PM emissions and the relative emission fractions of Aitken- and accumulation-mode PM, large uncertainties in the parameterizations of homogeneous nucleation used in 3-D air quality model and the numerical algorithms of other important processes in determining PM number and mass concentrations such as coagulation and other gas-to-particle conversion processes (e.g., diffusion, condensation, heterogeneous reactions), uncertainties associated with important model parameters such as initial PM size distribution, uncertainties in the model treatment of nanoparticle growth to the CCN size, as well as lack of measurements (e.g., the size resolved number, mass, and surface area concentrations of PM and the corresponding concentrations of gas precursors of secondary PM such as SO_2, NO_x, NH_3, H_2SO_4, HNO_3, and VOCs) at sites representative of various ambient atmospheric meteorological and chemical conditions for model/parameterization validation. Extra cautions are advised in selecting a homogeneous nucleation parameterization since most parameterizations have not been rigorously tested for all ranges of ambient conditions and the appropriateness of one parameterization cannot be determined solely based on whether it gives a good agreement with observations. The model evaluation conducted here is based on a horizontal grid resolution of 32 km and uses observational data at only one urban location. Given large differences in the controlling processes for PM number, volume, and surface area predictions between urban/upwind locations and nonurban/downwind locations, the performance of various nucleation parameterizations against observations may vary, depending on characteristics of emissions, meteorology, topography of those locations, as well as the grid resolution used for model simulations. The evaluation results from the calculations of *Zhang et al.* [2010b] and the 3-D model simulations in this paper are fairly consistent. They indicate that among the current parameterizations that are based on binary, ternary, kinetic, and cluster-activated nucleation theories, those of *Sihto et al.* [2006], *Kuang et al.* [2008], and *Harrington and Kreidenweis* [1998] perform better in the polluted boundary layer than most other parameterizations. Although *Napari et al.* [2002] also give a good agreement with observations under a sulfate-rich urban environment, their parameterization should not be continuously used because of several fundamental problems associated with it. As discussed previously, CMAQ does not simulate the growth of nanoparticle to the Aitken mode, which will introduce a large uncertainty. It is therefore important to develop such a growth module and couple it with a nucleation parameterization to reduce the uncertainty and improve the model's capability in simulating PM number concentrations and size distributions.

[30] **Acknowledgments.** This work was supported by the NSF award Atm-0348819, the NOAA award NA03NES4400015 and the Memorandum of Understanding between the U.S. Environmental Protection Agency (EPA) and the U.S. Department of Commerce's National Oceanic and Atmospheric Administration (NOAA) and under agreement DW13921548, and the National Research Initiative Competitive Grant 2008-35112-18758 from the USDA Cooperative State Research, Education, and Extension Service Air Quality Program at North Carolina State University. P.H.M. was supported by NSF award ATM-0506674. F.Y. acknowledges support from NSF award AGS-0942106. Thanks are owed to Hanna Vehkamäki, University of Helsinki, Finland, for providing a corrected version of code for *Merikanto et al.*'s [2007] parameterization, Alan Hansen, EPRI, for permitting the use of the ARIES PM number and size distribution data for model evaluation, Prakash V. Bhave, U.S. EPA, for helpful discussions during an early stage of this work, and Kai Wang, NCSU, for help in postprocessing process analysis results. Although this work was reviewed by EPA and approved for publication, it does not necessarily reflect their policies or views.

References

Anttila, T., H. Vehkamäki, I. Napari, and M. Kulmala (2005), Effect of ammonium bisulphate formation on atmospheric water-sulphuric acid-ammonia nucleation, *Boreal Environ. Res.*, *10*, 511–523.

Binkowski, F. S., and S. J. Roselle (2003), Models-3 Community Multiscale Air Quality (CMAQ) model aerosol component: 1. Model description, *J. Geophys. Res.*, *108*(D6), 4183, doi:10.1029/2001JD001409.

Blando, J. D., R. J. Porcja, T. H. Li, D. Bowman, P. J. Lioy, and B. Turpin (1998), Secondary formation and the Smoky Mountain organic aerosol: An examination of aerosol polarity and functional group composition during SEAVS, *Environ. Sci. Technol.*, *32*, 604–613, doi:10.1021/es970405s.

Byun, D., and K. L. Schere (2006), Review of the governing equations, computational algorithms, and other components of the Models-3 Community Multiscale Air Quality (CMAQ) modeling system, *Appl. Mech. Rev.*, *59*, 51–77, doi:10.1115/1.2128636.

Carter, W. P. L. (2000), Implementation of the SAPRC99 chemical mechanism into the Models-3 Framework, Report to the US Environmental Agency, ftp://ftp.cert.ucr.edu/pub/carter/pubs/s99mod3.pdf.

Day, D. E., W. C. Malm, and S. M. Kreidenweis (1997), Seasonal variations in aerosol composition and acidity at Shenandoah and Great Smoky Mountains National Parks, *J. Air and Waste Manage. Assoc.*, *47*, 411–418.

Eisele, F. L., and P. H. McMurry (1997), Recent progress in understanding particle nucleation and growth, *Philos. Trans. R. Soc. B*, *352*, 191–201, doi:10.1098/rstb.1997.0014.

Elleman, R. A., and D. S. Covert (2009a), Aerosol size distribution modeling with the Community Multiscale Air Quality modeling system in the Pacific Northwest: 1. Model comparison to observations, *J. Geophys. Res.*, *114*, D11206, doi:10.1029/2008JD010791.

Elleman, R. A., and D. S. Covert (2009b), Aerosol size distribution modeling with the Community Multiscale Air Quality modeling system in the Pacific Northwest: 2. Parameterizations for ternary nucleation and nucleation mode processes, *J. Geophys. Res.*, *114*, D11207, doi:10.1029/2009JD012187.

Elleman, R. A., and D. S. Covert (2010), Aerosol size distribution modeling with the Community Multiscale Air Quality modeling system in the Pacific Northwest: 3. Size distribution of particles emitted into a mesoscale model, *J. Geophys. Res.*, *115*, D03204, doi:10.1029/2009JD012401.

Fitzgerald, J. W., W. A. Hoppel, and F. Gelbard (1998), A one-dimensional sectional model to simulate multicomponent aerosol dynamics in the marine boundary layer. 1. Modal description, *J. Geophys. Res.*, *103*, 16,085–16,102, doi:10.1029/98JD01019.

Gaydos, T. M., C. O. Stanier, and S. N. Pandis (2005), Modeling of in situ ultrafine atmospheric particle formation in the eastern United States, *J. Geophys. Res.*, *110*, D07S12, doi:10.1029/2004JD004683.

Harrington, D. Y., and S. M. Kreidenweis (1998), Simulation of sulfate aerosol dynamics. I. Model description, *Atmos. Environ.*, *32*, 1691–1700, doi:10.1016/S1352-2310(97)00452-4.

Jacobson, M. Z. (1999), Studying the effects of calcium and magnesium on size-distributed nitrate and ammonium with EQUISOLV II, *Atmos. Environ.*, *33*, 3635–3649, doi:10.1016/S1352-2310(99)00105-3.

Jung, J. G., S. N. Pandis, and P. J. Adams (2008), Evaluation of nucleation theories in a sulfur-rich environment, *Aerosol Sci. Technol.*, *42*, 495–504, doi:10.1080/02786820802187085.

Jung, J., C. Fountoukis, P. J. Adams, and S. N. Pandis (2010), Simulation of in situ ultrafine particle formation in the eastern United States using PMCAMx-UF, *J. Geophys. Res.*, *115*, D03203, doi:10.1029/2009JD012313.

Kavouras, I. G., N. Mihalopoulos, and E. G. Stephanou (1998), Formation of atmospheric particles from organic acids produced by forests, *Nature*, *395*, 683–686, doi:10.1038/27179.

Kerminen, V. M., and M. Kulmala (2002), Analytical formulae connecting the "real" and the "apparent" nucleation rate and the nuclei number concentration for atmospheric nucleation events, *J. Aerosol Sci.*, *33*(4), 609–622, doi:10.1016/S0021-8502(01)00194-X.

Korhonen, H., K. S. Carslaw, D. V. Spracklen, D. A. Ridley, and J. Ström (2008), A global model study of processes controlling aerosol size distributions in the Arctic spring and summer, *J. Geophys. Res.*, *113*, D08211, doi:10.1029/2007JD009114.

Kuang, C., P. H. McMurry, A. V. McCormick, and F. L. Eisele (2008), Dependence of nucleation rates on sulfuric acid vapor concentration in diverse atmospheric locations, *J. Geophys. Res.*, *113*, D10209, doi:10.1029/2007JD009253.

Kuang, C., P. H. McMurry, and A. V. McCormick (2009), Determination of cloud condensation nuclei production from measured new particle formation events, *Geophys. Res. Lett.*, *36*, L09822, doi:10.1029/2009GL037584.

Kulmala, M., A. Laaksonen, and L. Pirjola (1998), Parameterizations for sulphuric acid/water nucleation rates, *J. Geophys. Res.*, *103*, 8301–8307, doi:10.1029/97JD03718.

Kulmala, M., L. Pirjola, and J. M. Mäkelä (2000), Stable sulphate clusters as a source of new atmospheric particles, *Nature*, *404*, 66–69, doi:10.1038/35003550.

Kulmala, M., L. Laakso, K. E. J. Lehtinen, I. Riipinen, M. Dal Maso, T. Anttila, V.-M. Kerminen, U. Hõrrak, M. Vana, and H. Tammet (2004a), Initial steps of aerosol growth, *Atmos. Chem. Phys.*, *4*, 2553–2560, doi:10.5194/acp-4-2553-2004.

Kulmala, M., H. Vehkamäki, T. Petäjä, M. Dal Maso, A. Lauri, V.-M. Kerminen, W. Birmili, and P. H. McMurry (2004b), Formation and growth rates of ultrafine atmospheric particles: A review of observations, *J. Aerosol Sci.*, *35*, 143–176, doi:10.1016/j.jaerosci.2003.10.003.

Liu, P., and Y. Zhang (2010), Use of a process analysis tool for diagnostic study on fine particulate matter predictions in the U.S. Part I: Model evaluation using surface, aircraft, and satellite data, *Atmos. Pollut. Res.*, in press.

Liu, P., Y. Zhang, S. C. Yu, and K. L. Schere (2010), Use of a process analysis tool for diagnostic study on fine particulate matter predictions in the U.S. Part II: Process analyses and sensitivity simulations, *Atmos. Pollut. Res.* , in press.

Liu, X.-H., Y. Zhang, J. Xing, Q. Zhang, D. G. Streets, C. J. Jang, W.-X. Wang, and J.-M. Hao (2010a), Understanding of regional air pollution over China using CMAQ - Part II. Process analysis and ozone sensitivity to precursor emissions, *Atmos. Environ.*, *44*, 3719–3727, doi:10.1016/j.atmosenv.2010.03.036.

Liu, X.-H., Y. Zhang, J. Xing, Q. Zhang, D. G. Streets, C. J. Jang, W.-X. Wang, and J.-M. Hao (2010b), Understanding of regional air pollution over China using CMAQ - Part I. Performance evaluation and seasonal variation, *Atmos. Environ.*, *44*, 2415–2426, doi:10.1016/j.atmosenv.2010.03.035.

Lucas, D. D., and H. Akimoto (2006), Evaluating aerosol nucleation parameterizations in a global atmospheric model, *Geophys. Res. Lett.*, *33*, L10808, doi:10.1029/2006GL025672.

Malm, W. C. (1979), Considerations in the measurements of visibility, *J. Air Pollut. Control Assoc.*, *29*, 1042–1052.

McMurry, P. H. (1980), Photochemical aerosol formation from SO_2: A theoretical analysis of smog chamber data, *J. Colloid Interface Sci.*, *78*, 513–527, doi:10.1016/0021-9797(80)90589-5.

McMurry, P. H. (1983), New particle formation in the presence of an aerosol: Rates, time scales, and sub −0.01 μm size distributions, *J. Colloid Interface Sci.*, *95*, 72–80, doi:10.1016/0021-9797(83)90073-5.

McMurry, P. H., and K. S. Woo (2002), Size distributions of 3–100-nm urban Atlanta aerosols: Measurement and observations, *J. Aerosol Med.*, *15*(2), 169–178, doi:10.1089/089426802320282293.

McMurry, P. H., K. S. Woo, R. Weber, D.-R. Chen, and D. Y. H. Pui (2000), Size distributions of 3–10 nm atmospheric particles: Implications for nucleation mechanisms, *Philos. Trans. R. Soc. A*, *358*, 2625–2642, doi:10.1098/rsta.2000.0673.

McMurry, P., M. Fink, H. Sakurai, M. Stolzenburg, L. Mauldin, K. Moore, J. Smith, F. Eisele, S. Sjostedt, and D. Tanner (2005), A criterion for new particle formation in the sulfur-rich Atlanta atmosphere, *J. Geophys. Res.*, *110*, D22S02, doi:10.1029/2005JD005901.

Merikanto, J., E. Zapadinsky, A. Lauri, and H. Vehkamäki (2007), Origin of the failure of classical nucleation theory: Incorrect description of the smallest clusters, *Phys. Rev. Lett.*, *98*, 145702, doi:10.1103/PhysRevLett.98.145702.

Merikanto, J., D. V. Spracklen, G. W. Mann, S. J. Pickering, and K. S. Carslaw (2009a), Impact of nucleation on global CCN, *Atmos. Chem. Phys.*, *9*, 8601–8616, doi:10.5194/acp-9-8601-2009.

Merikanto, J., I. Napari, H. Vehkamäki, T. Anttila, and M. Kulmala (2009b), Correction to "New parameterization of sulfuric acid-ammonia-water ternary nucleation rates at tropospheric conditions," *J. Geophys. Res.*, *114*, D09206, doi:10.1029/2009JD012136.

Napari, I., M. Noppel, H. Vehkamäki, and M. Kulmala (2002), Parameterization of ternary nucleation rates for H_2SO_4-NH_3-H_2O vapors, *J. Geophys. Res.*, *107*(D19), 4381, doi:10.1029/2002JD002132.

Noppel, M., H. Vehkamäki, and M. Kulmala (2002), An improved model for hydrate formation in sulfuric acid-water nucleation, *J. Chem. Phys.*, *116*, 218–228, doi:10.1063/1.1423333.

O'Halloran, T. L., J. D. Fuentes, D. R. Collins, M. J. Cleveland, and W. C. Keene (2009), Influence of air mass source region on nanoparticle events and hygroscopicity in central Virginia, *U.S., Atmos. Environ.*, *43*, 3586–3595, doi:10.1016/j.atmosenv.2009.03.033.

Pandis, S. N., L. M. Russell, and J. H. Seinfeld (1994), The relationship between DMS flux and CCN concentration in remote marine regions, *J. Geophys. Res.*, *99*, 16,945–16,957, doi:10.1029/94JD01119.

Park, S.-K., A. Marmur, S. B. Kim, D. Tian, Y. Hu, P. H. McMurry, and A. G. Russell (2006), Evaluation of fine particle number concentrations in CMAQ, *Aerosol Sci. Technol.*, *40*, 985–996, doi:10.1080/02786820600907353.

Pierce, J. R., and P. J. Adams (2007), Efficiency of cloud condensation nuclei formation from ultrafine particles, *Atmos. Chem. Phys.*, *7*, 1367–1379, doi:10.5194/acp-7-1367-2007.

Pierce, J. R., and P. J. Adams (2009), Uncertainty in global CCN concentrations from uncertain aerosol nucleation and primary emission rate, *Atmos. Chem. Phys.*, *9*, 1339–1356, doi:10.5194/acp-9-1339-2009.

Pleim, J., D. Wong, R. Mathur, J. Young, T. Otte, R. Gilliam, F. Binkowski, and A. Xiu (2008), Development of the coupled 2-way WRF-CMAQ system, paper presented at 2008 Annual CMAS Conference, CMAS Cent., Research Triangle Park, N. C.

Roth, H., W. Jiang, D. Yin, and E. Giroux (2003), CMAQ nucleation algorithms and their impact on PM modeling results in the lower Fraser Valley, paper presented at 2003 CMAS Models-3 User's Workshop: One Atmosphere, One Community, One Modeling System: Models-3, CMAS Cent., Research Triangle Park, N. C.

Seinfeld, J. H., and S. N. Pandis (2006), *Atmospheric Chemistry and Physics: From Air Pollution to Climate Change*, 2nd ed., 1232 pp., John Wiley, Hoboken, N. J.

Sihto, S., M. Kulmala, V. Kerminen, M. Dal Maso, T. Petäjä, I. Riipinen, H. Korhonen, F. Arnold, R. Janson, and M. Boy (2006), Atmospheric sulphuric acid and aerosol formation: Implications from atmospheric measurements for nucleation and early growth mechanisms, *Atmos. Chem. Phys.*, *6*, 4079–4091, doi:10.5194/acp-6-4079-2006.

Smith, J. N., M. J. Dunn, T. M. VanReken, K. Iida, M. R. Stolzenburg, P. H. McMurry, and L. G. Huey (2008), Chemical composition of atmospheric nanoparticles formed from nucleation in Tecamac, Mexico: Evidence for an important role for organic species in nanoparticle growth, *Geophys. Res. Lett.*, *35*, L04808, doi:10.1029/2007GL032523.

Smith, J. N., K. C. Barsanti, H. R. Friedli, M. Ehn, M. Kulmala, D. R. Collins, J. H. Scheckman, B. J. Williams, and P. H. McMurry (2010), Observations of aminium salt formation in atmospheric nanoparticles and possible climatic implications, *Proc. Natl. Acad. Sci. U. S. A.*, *107*(15), 6634–6639, doi:10.1073/pnas.0912127107.

Spracklen, D. V., K. J. Pringle, K. S. Carslaw, M. P. Chipperfield, and G. W. Mann (2005), A global off-line model of size-resolved aerosol microphysics: I. Model development and prediction of aerosol properties, *Atmos. Chem. Phys.*, *5*, 2227–2252, doi:10.5194/acp-5-2227-2005.

Spracklen, D. V., K. S. Carslaw, M. Kulmala, V.-M. Kerminen, G. W. Mann, and S.-L. Sihto (2006), The contribution of boundary layer nucleation events to total particle concentrations on regional and global scales, *Atmos. Chem. Phys.*, *6*, 5631–5648, doi:10.5194/acp-6-5631-2006.

Spracklen, D. V., K. J. Pringle, K. S. Carslaw, G. W. Mann, P. Manktelow, and J. Heintzenberg (2007), Evaluation of a global aerosol microphysics model against size-resolved particle statistics in the marine atmosphere, *Atmos. Chem. Phys.*, *7*, 2073–2090, doi:10.5194/acp-7-2073-2007.

Spracklen, D. V., et al. (2008), Contribution of particle formation to global cloud condensation nuclei concentrations, *Geophys. Res. Lett.*, *35*, L06808, doi:10.1029/2007GL033038.

Van Loy, M., T. Bahadori, R. Wyzga, B. Hartsell, and E. Ederton (2000), The aerosol research and inhalation epidemiology study (ARIES): PM2.5 mass and aerosol component concentrations and sampler intercomparisons, *J. Air Waste Manage. Assoc.*, *50*, 1446–1458.

Vehkamäki, H., M. Kulmala, I. Napari, K. E. J. Lehtinen, C. Timmreck, M. Noppel, and A. Laaksonen (2002), An improved parameterization for sulfuric acid-water nucleation rates for tropospheric and stratospheric conditions, *J. Geophys. Res.*, *107*(D22), 4622, doi:10.1029/2002JD002184.

Wang, K., Y. Zhang, C. J. Jang, S. Phillips, and B.-Y. Wang (2009), Modeling study of intercontinental air pollution transport over the trans-Pacific region in 2001 using the Community Multiscale Air Quality (CMAQ) modeling system, *J. Geophys. Res.*, *114*, D04307, doi:10.1029/2008JD010807.

Wexler, A. S., F. W. Lurmann, and J. H. Seinfeld (1994), Modeling urban and regional aerosols. I. Model development, *Atmos. Environ.*, *28*, 531–546, doi:10.1016/1352-2310(94)90129-5.

Whitby, K. T. (1978), The physical characteristics of sulfate aerosols, *Atmos. Environ.*, *12*, 135–159.

Woo, K. S. (2003), Measurement of atmospheric aerosols: Size distributions of nanoparticles, estimation of size distribution moments and con-

trol of relative humidity, Ph.D. thesis, Dep. of Mech. Eng., Univ. of Minn. Twin Cities, Minneapolis.

Woo, K. S., D. R. Chen, D. Y. H. Pui, and P. H. McMurry (2001), Measurement of Atlanta aerosol size distributions: Observations of ultrafine particle events, *Aerosol Sci. Technol.*, *34*, 75–87, doi:10.1080/027868201300082049.

Yu, F. (2006), Effect of ammonia on new particle formation: A kinetic H_2SO_4-H_2O-NH_3 nucleation model constrained by laboratory measurements, *J. Geophys. Res.*, *111*, D01204, doi:10.1029/2005JD005968.

Yu, F. (2008), Updated H_2SO_4–H_2O binary homogeneous nucleation rate look-up tables, *J. Geophys. Res.*, *113*, D24201, doi:10.1029/2008JD010527.

Yu, F., and G. Luo (2009), Simulation of particle size distribution with a global aerosol model: Contribution of nucleation to aerosol and CCN number concentrations, *Atmos. Chem. Phys.*, *9*, 7691–7710, doi:10.5194/acp-9-7691-2009.

Yu, F., G. Luo, T. S. Bates, B. Anderson, A. Clarke, V. Kapustin, B. Yantosca, Y.-X. Wang, and S.-L. Wu (2010), Spatial distributions of particle number concentrations in the global troposphere: Simulations, observations, and implications for nucleation mechanisms, *J. Geophys. Res.*, *115*, D17205, doi:10.1029/2009JD013473.

Yu, S., R. L. Dennis, P. V. Bhave, and B. K. Eder (2004), Primary and secondary organic aerosols over the United States: Estimates on the basis of observed organic carbon (OC) and elemental carbon (EC), and air quality modeled primary OC/EC ratios, *Atmos. Environ.*, *38*, 5257–5268, doi:10.1016/j.atmosenv.2004.02.064.

Yu, S. C., B. Eder, R. Dennis, S.-H. Chu, and S. Schwartz (2006), New unbiased symmetric metrics for evaluation of air quality models, *Atmos. Sci. Lett.*, *7*, 26–34, doi:10.1002/asl.125.

Yu, S.-C., R. Mathur, K. Schere, D. Kang, J. Pleim, J. Young, D. Tong, G. Pouliot, S. A. McKeen, and S. T. Rao (2008), Evaluation of real-time PM forecasts and process analysis for PM formation over the eastern United States using the Eta-CMAQ forecast model during the 2004 ICARTT study, *J. Geophys. Res.*, *113*, D06204, doi:10.1029/2007JD009226.

Zhang, R., I. Suh, J. Zhao, D. Zhang, E. C. Fortner, X. Tie, L. T. Molina, and M. J. Molina (2004), Enhanced atmospheric new particle formation by organic acids, *Science*, *304*, 1487–1490, doi:10.1126/science.1095139.

Zhang, Y. (2008), Online coupled meteorology and chemistry models: History, current status, and outlook, *Atmos. Chem. Phys.*, *8*, 2895–2932, doi:10.5194/acp-8-2895-2008.

Zhang, Y., and M. Z. Jacobson (2005), A comparative study of nucleation parameterizations for 3-D atmospheric models, paper presented at 9th Atmospheric Sciences and Air Quality Conference, Am. Meteorol. Soc., San Francisco, Calif.

Zhang, Y., C. Seigneur, J. H. Seinfeld, M. Z. Jacobson, and F. S. Binkowski (1999), Simulation of aerosol dynamics), A comparative review of algorithms used in air quality models, *Aerosol Sci. Technol.*, *31*, 487–514, doi:10.1080/027868299304039.

Zhang, Y., K. Vijayaraghavan, and C. Seigneur (2005), Evaluation of three probing techniques in a three-dimensional air quality model, *J. Geophys. Res.*, *110*, D02305, doi:10.1029/2004JD005248.

Zhang, Y., P. Liu, B. Pun, and C. Seigneur (2006), A comprehensive performance evaluation of MM5-CMAQ for summer 1999 southern oxidants study episode, Part III. Diagnostic and mechanistic evaluations, *Atmos. Environ.*, *40*, 4856–4873, doi:10.1016/j.atmosenv.2005.12.046.

Zhang, Y., J.-P. Huang, D. K. Henze, and J. H. Seinfeld (2007), The role of isoprene in secondary organic aerosol formation on a regional scale, *J. Geophys. Res.*, *112*, D20207, doi:10.1029/2007JD008675.

Zhang, Y., Y.-S. Chen, P. Pillai, and X.-Y. Dong (2009a), Sensitivity of simulated aerosol and cloud properties to nucleation parameterizations in 3-D regional and global models, paper presented at 28th Annual Meeting, AAAR, Minneapolis, Minn.

Zhang, Y., X.-Y. Wen, K. Wang, K. Vijayaraghavan, and M. Z. Jacobson (2009b), Probing into regional O_3 and PM pollution in the United States: 2. An examination of formation mechanisms through a process analysis technique and sensitivity study, *J. Geophys. Res.*, *114*, D22305, doi:10.1029/2009JD011900.

Zhang, Y., P. Liu, X.-H. Liu, B. Pun, C. Seigneur, M. Z. Jacobson, and W.-X. Wang (2010a), Fine-scale modeling of wintertime aerosol mass, number, and size distributions in central California, *J. Geophys. Res.*, *115*, D15207, doi:10.1029/2009JD012950.

Zhang, Y., P. H. McMurry, F. Yu, and M. Z. Jacobson (2010b), A comparative study of homogeneous nucleation parameterizations: 1. Examination and evaluation of the formulations, *J. Geophys. Res.*, *115*, D20212, doi:10.1029/2009JD014150.

M. Z. Jacobson, Department of Civil and Environmental Engineering, Stanford University, Stanford, CA 94305, USA.

P. Liu, X.-H. Liu, and Y. Zhang, Department of Marine, Earth, and Atmospheric Sciences, North Carolina State University, Campus Box 8208, Raleigh, NC 27695, USA. (yang_zhang@ncsu.edu)

P. H. McMurry, Department of Mechanical Engineering, University of Minnesota-Twin Cities, Minneapolis, MN 55455, USA.

K. L. Schere and S. Yu, Atmospheric Modeling and Analysis Division, U.S. Environmental Protection Agency, Research Triangle Park, NC 27711, USA.

F. Yu, Atmospheric Sciences Research Center, State University of New York at Albany, Albany, NY 12222, USA.